

Transformation graphene quantum dot structure on Ag
electrodes under electrochemical reduction.



Mr. Sivakorn Bovornsintuchon

จุฬาลงกรณ์มหาวิทยาลัย
CHULALONGKORN UNIVERSITY

A Thesis Submitted in Partial Fulfillment of the Requirements
for the Degree of Master of Engineering in Chemical Engineering
Department of Chemical Engineering
Faculty Of Engineering
Chulalongkorn University
Academic Year 2023

การเปลี่ยนแปลงโครงสร้างของแกรฟีนควอนตัมคอปบนจิวซิลเวอร์อิเล็กโทรดภายใต้การรีดักชัน
แบบไฟฟ้าเคมี



วิทยานิพนธ์นี้เป็นส่วนหนึ่งของการศึกษาตามหลักสูตรปริญญาวิศวกรรมศาสตรมหาบัณฑิต
สาขาวิชาวิศวกรรมเคมี ภาควิชาวิศวกรรมเคมี
คณะวิศวกรรมศาสตร์ จุฬาลงกรณ์มหาวิทยาลัย
ปีการศึกษา 2566

Thesis Title Transformation graphene quantum dot structure on Ag electrodes under electrochemical reduction.
By Mr. Sivakorn Bovornsintuchon
Field of Study Chemical Engineering
Thesis Advisor Professor JOONGJAI PANPRANOT, Ph.D.

Accepted by the FACULTY OF ENGINEERING, Chulalongkorn University
in Partial Fulfillment of the Requirement for the Master of Engineering

..... Dean of the FACULTY OF
ENGINEERING
(Professor SUPOT TEACHAVORASINSKUN, D.Eng.)

THESIS COMMITTEE

..... Chairman
(Professor PAISAN KITTISUPAKORN, Ph.D.)
..... Thesis Advisor
(Professor JOONGJAI PANPRANOT, Ph.D.)
..... Examiner
(Professor ARTIWAN SHOTIPRUK, Ph.D.)
..... External Examiner
(Assistant Professor Patcharaporn Weerachawanasak,
D.Eng.)



จุฬาลงกรณ์มหาวิทยาลัย
CHULALONGKORN UNIVERSITY

ศิวกร บวรสินธุชด : การเปลี่ยนแปลงโครงสร้างของแกรฟีนควอนตัมคอตบนขั้วซิลเวอร์
อิเล็กโทรดภายใต้การรีดักชันแบบไฟฟ้าเคมี. (Transformation graphene
quantum dot structure on Ag electrodes under electrochemical
reduction.) อ.ที่ปรึกษาหลัก : ศ.จุงใจ ปั้นประณต

ในงานนี้เป็นการศึกษาผลของเวลาในการรีดักชันทางไฟฟ้าเคมีต่อการเปลี่ยนแปลงโครงสร้างของแกรฟีนควอนตัมคอต (GQDs) บนขั้วซิลเวอร์อิเล็กโทรด ภายใต้การรีดักชันแบบไฟฟ้าเคมี ซึ่งเตรียมโดยการนำ GQDs ที่ได้จากสารตั้งต้นสามชนิดคือ Acetic , Glycine และ Bicarbonate มาผ่านกระบวนการรีดักชันทางไฟฟ้าเคมีบนขั้วซิลเวอร์/ทองแดง ที่เวลาตั้งแต่ 15, 30, 45 และ 60 นาที ตัวอย่าง GQDs ที่ได้จากการเปลี่ยนแปลงโครงสร้างโดยวิธีรีดักชันทางไฟฟ้าเคมีและนำตัวอย่างในแต่ละช่วงเวลามานำไปทดสอบการประยุกต์ใช้ในการคัดแปรขั้วไฟฟ้าคาร์บอนพิมพ์สกรีน แกรฟีน โดยโดยใช้เทคนิคไซคลิกโวลแทมเมตรี จากผลการทดสอบไซคลิกโวลแทมเมตรี พบว่า จากตัวอย่างทั้งหมด ตัวอย่างที่ได้จาก Blue CL- GQDs #Acetic ที่ทำปฏิกิริยาเป็นเวลา 15 นาที และ 60 นาที ให้กระแสสูงที่สุดและ เมื่อเทียบกับ GQD ที่ได้จาก Blue CL- GQDs #Glycine และ Yellow CL- GQDs #Bicarbonate และขั้วที่ไม่มีการคัดแปร (Unmodified SPCE) เหมาะสำหรับการใช้กับขั้วไฟฟ้าพิมพ์สกรีน (screen-printed electrode) เนื่องจากเมื่อสังเกตจากผลจากกล้องจุลทรรศน์อิเล็กตรอนแบบส่องกราดและเอินเนอซีดีสเพอซิฟิเคชันสเปกโทรสโกปี (SEM-EDX) พบว่า ลักษณะโครงสร้างเป็นรูปแบบฟิล์มบาง (smooth thin film) และโครงสร้างแบบ มีความเป็น sp^2 ซึ่งมีพันธะอะตอมแบบ พันธะคู่ (double bonds) โดยจะช่วยให้มีอิเล็กตรอนเคลื่อนที่ได้ดีกว่าโครงสร้างแบบ sp^3 ที่มีพันธะอะตอมแบบ single bonds ทำให้ GQDs ที่มีโครงสร้างที่เป็น sp^2 สามารถนำไฟฟ้าได้ดีมากกว่าเนื่องจากอิเล็กตรอนสามารถเคลื่อนที่ได้ไหลผ่านโครงสร้างนี้ได้โดยอิสระมากขึ้น อย่างไรก็ตามสมบัติการนำไฟฟ้า ไม่ขึ้นกับรูปร่างแบบ 2D หรือ 3D ของ GQDs มากนัก แต่ขึ้นกับอัตราส่วน sp^2/sp^3 และ ความกราฟิติกเป็นหลัก

สาขาวิชา วิศวกรรมเคมี

ลายมือชื่อนิติ

ปีการศึกษา 2566

ลายมือชื่อ อ.ที่ปรึกษาหลัก

6370277521 : MAJOR CHEMICAL ENGINEERING

KEYWORD Cyclic voltammetry (CV), Graphene quantum dot (GQDs), Graphene screen print electrode

Sivakorn Bovornsintuchon : Transformation graphene quantum dot structure on Ag electrodes under electrochemical reduction.. Advisor: Prof. JOONGJAI PANPRANOT, Ph.D.

In this study, we investigated the effect of electrochemical reduction time on the characteristics structural changes of various GQDs on Ag/Cu electrode was investigated. The GQDs were derived from three precursors including materials: Acetic, Glycine, and Bicarbonate were treated under electrochemical reduction conditions for , with reaction times of 15, 30, 45, and 60 minutes respectively. The obtained sSamples from each time period were then tested for their applicability in graphene screen-printed carbon electrodes using cyclic voltammetry techniques. The cyclic voltammetry test results revealed that among all the samples, those derived from Blue CL-GQDs #Acetic at 15 minutes and 60 minutes exhibited the highest current compared to GQDs obtained from Blue CL-GQDs #Glycine, Yellow CL-GQDs #Bicarbonate, and unmodified terminals. These samples proved suitable for use with screen-printed electrodes. Observing the SEM-EDX results showed that the structure appears as a smooth, thin film structure with an sp^2 hybridization structure characterized by double atomic bonds, enabling the presence of more excess electrons provide higher conductivity than the sp^3 structure with single atomic bonds. This characteristic facilitates better electrical conductivity as electrons can move more freely through this structure. However, the conductivity of GQDs does not depend much on the 2D or 3D structure but is rather affected by the sp^2/sp^3 ratios and the graphitic content.



Field of Study: Chemical Engineering

Student's Signature

Academic Year: 2023

Advisor's Signature

Year:

.....

ACKNOWLEDGEMENTS

I am much admired my advisor, Prof. Dr. Joongjai Panpranot. She has provided advice, counselling, assistance, and motivation for my thesis since start to first study until last semester to prepare thesis's defense exam, Thank you to Crystallyte co., ltd. that provided the location for the lab as well as budget support in this research. Besides, I am appreciative to Professor Paisan Kittisupakorn, Ph.D, as the chairman, Professor Artiwan Shotipruk, Ph.D. and Dr. Patcharaporn Weerachawanasak as an examiner of the committee group for their significant guidance and recommendation on this thesis.

Moreover, I am impressed to my parents and my friends for give me a helpful and many valuable suggestions when I faced with stress and many problem.

Sivakorn Bovornsintuchon

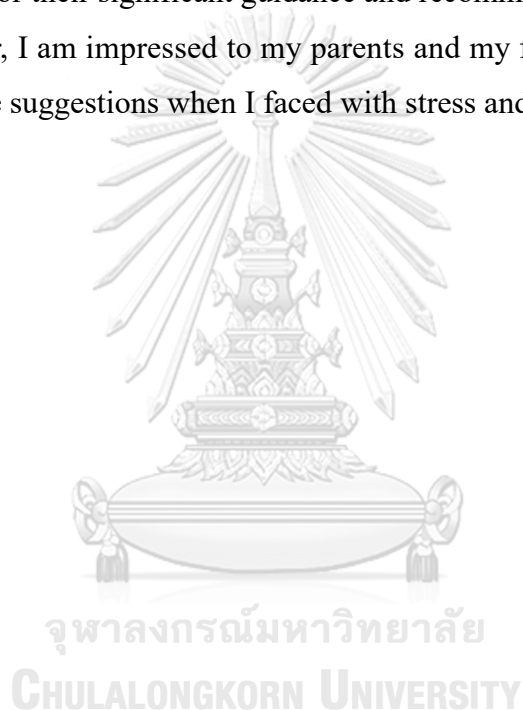


TABLE OF CONTENTS

	Page
.....	iii
ABSTRACT (THAI)	iii
.....	iv
ABSTRACT (ENGLISH).....	iv
ACKNOWLEDGEMENTS.....	v
TABLE OF CONTENTS.....	vi
LIST OF TABLES	ix
LIST OF FIGURES	x
LIST OF TABLES	1
LIST OF FIGURES	2
CHAPTER I.....	4
INTRODUCTION	4
1.1 Introduction.....	4
1.2 Objectives of the Research	5
1.3 Scopes of the Research.....	5
CHAPTER II.....	1
BACKGROUND AND LITERATURE REVIEWS.....	1
2.1 Properties of graphene quantum dot.....	1
2.1.1 Physical Properties	1
2.1.2 Electrochemical Properties.....	1
2.2 Electrodeposition of Ag electrocatalysts.	2
2.3 Cyclic voltammetry (CV)	2
2.4 Screen-printed electrodes (SPEs)	3
2.5 Fluorescent mechanism carbon dots.....	4
2.5.1 Quantum confinement.....	4

2.6 Raman spectroscopy	6
2.7 Scanning electron microscope	6
2.8 X-ray photoelectron spectroscopy	7
CHAPTER III	8
MATERIALS AND METHODS	8
3.1 Materials	8
3.2 Catalysts preparation	8
3.2.1 Preparation of electrodes	8
3.2.2 Preparation of Ag catalysts (Ag/Cu).....	8
3.3 Electrochemical transformation structure experiment of graphene quantum dots	9
3.4 Characterization.....	10
3.3.1 Scanning electron microscope-energy dispersive X-ray spectroscopy (SEM-EDX).....	10
3.3.2 X-ray Photoelectron Spectroscopy (XPS).....	10
3.3.3 Raman Spectroscopy	10
3.5 Electrochemical Sensor	11
3.6 Research methodology	12
CHAPTER IV	14
RESULTS AND DISCUSSION.....	14
4.1 Characterization of the sample by Scanning electron microscope-energy dispersive X-ray spectroscopy (SEM-EDX)	14
4.1.1 Scanning electron microscope-energy dispersive X-ray spectroscopy (SEM-EDX) of Blue CL- GQDs #Acetic different times (15, 30, 45 and 60 min.)	14
4.2 Characterization of the sample by X-ray Photoelectron Spectroscopy (XPS) ..	23
4.2.1 X-ray Photoelectron Spectroscopy of Blue CL- GQDs #Acetic different times (5, 30, 45 and 60 min.).....	23
4.3 Characterization of the sample by Raman spectroscopy	32
4.3.1 Raman spectroscopy of Blue CL- GQDs #Acetic different times (5, 30, 45 and 60 min.).....	32

4.3.2 Raman spectroscopy of Blue CL- GQDs #Glycine different times (5, 30, 45 and 60 min.).....	35
4.4 Electrochemical characterization of GQDs	42
4.4.1 Application of Blue CL- GQDs #Acetic, Derived transforming graphene quantum dot structure on Ag electrodes under electrochemical reduction in Electrochemical Sensor	42
CHAPTER V	48
CONCLUSIONS.....	48
5.1 Conclusions	48
5.2 Recommendations	49
REFERENCES	50
VITA	52



LIST OF TABLES

Page

No table of figures entries found.



LIST OF FIGURES

Page

No table of figures entries found.



LIST OF TABLES

	Page
Table 1 Chemicals used as precursors and electrolyte.....	8
Table 2 Metals used as electrodes in electrodeposition method.	8
Table 3 Code for calling the sample in each condition.	13
Table 4 Table for comparison all of condition Carbon (C) percent by atom and particle size of Blue CL- GQDs #Acetic.	16
Table 5 Table for comparison all of condition Carbon (C) percent by atom and particle size of Blue CL- GQDs # Glycine.	19
Table 6 Table for comparison all of condition Carbon (C) percent by atom and particle size of Blue CL- GQDs # Glycine.	22
Table 7 Contribution of carbon states to the total C 1s spectrum (%) in transformation Blue CL- GQDs #Acetic structure on Ag electrodes under electrochemical reduction.	25
Table 8 Contribution of carbon states to the total C 1s spectrum (%) in transformation Blue CL- GQDs #Glycine structure on Ag electrodes under electrochemical reduction.	28
Table 9 Contribution of carbon states to the total C 1s spectrum (%) in transformation Yellow CL- GQDs #Bicarbonate structure on Ag electrodes under electrochemical reduction.	31
Table 10 IG/ID ratio of Blue CL- GQDs #Acetic.....	34
Table 11 IG/ID ratio of Blue CL- GQDs # Glycine.....	38
Table 12 IG/ID ratio of Blue CL- GQDs # Bicarbonate.....	41

LIST OF FIGURES

	Page
Figure 1 Electron arrangement of graphene.....	1
Figure 2 Cyclic voltammetry graph	2
Figure 3 Screen-printed electrode with the three electrodes system.....	3
Figure 4 Illustration of quantum confinement effect.	5
Figure 5 Analysis with a scanning electron microscope.....	7
Figure 6 Schematic of electrodeposition of Ag catalysts on different substrates.	9
Figure 7 Electrode positioning for electrochemical deformation experiment of graphene quantum dots.	10
Figure 8 Electrochemical Sensor testing.....	11
Figure 9 SEM-EDX images of Blue CL- GQDs #Acetic different times: (a) 15 minutes (b) 30 minutes (c) 45 minutes (d) 60 minutes	15
Figure 10 SEM-EDX images of Blue CL- GQDs #Glycine different times: (a) 15 minutes (b) 30 minutes (c) 45 minutes (d) 60 minutes	18
Figure 11 SEM-EDX images of Yellow CL- GQDs #Bicarbonate different times: (a) 15 minutes (b) 30 minutes (c) 45 minutes (d) 60 minutes	21
Figure 12 XPS image of Blue CL- GQDs #Acetic different times: (a) 15 minutes (b) 30 minutes (c) 45 minutes (d) 60 minutes	24
Figure 13 XPS image of Blue CL- GQDs #Glycine different times: (a) 15 minutes (b) 30 minutes (c) 45 minutes (d) 60 minutes	27
Figure 14 XPS image of Yellow CL- GQDs #Bicarbonate different times: (a) 15 minutes (b) 30 minutes (c) 45 minutes (d) 60 minutes	30
Figure 15 Raman spectroscopy image of Blue CL- GQDs #Acetic different times: (a) 15 minutes (b) 30 minutes (c) 45 minutes (d) 60 minutes	34
Figure 16 Raman spectroscopy image of Blue CL- GQDs #Glycine different times: (a) 15 minutes (b) 30 minutes (c) 45 minutes (d) 60 minutes.....	37
Figure 17 Raman spectroscopy image of Yellow CL- GQDs #Bicarbonate different times: (a) 15 minutes (b) 30 minutes (c) 45 minutes (d) 60 minute.	40
Figure 18 Illustration of Blue CL- GQDs #Acetic modified SPCE for electrochemical sensor application, Cyclic voltammograms of 5.0 mM $[\text{Fe}(\text{CN})_6]^{3-/4-}$ in 0.1 M KCl measured on different electrodes at a scan rate of 100 mVs^{-1} , and the corresponding peak current extracted from the CVs (n=3).	42

Figure 19 Illustration of Blue CL- GQDs #Acetic modified SPCE for electrochemical sensor application, show the current at potential 0.1 V	42
Figure 20 Illustration of Blue CL- GQDs #Acetic modified SPCE for electrochemical sensor application, show the current at potential -0.48 V	43
Figure 21 Illustration of Blue CL- GQDs #Glycine modified SPCE for electrochemical sensor application, Cyclic voltammograms of 5.0 mM $[\text{Fe}(\text{CN})_6]^{3-/4-}$ in 0.1 M KCl measured on different electrodes at a scan rate of 100 mVs^{-1} , and the corresponding peak current extracted from the CVs ($n=3$).	44
Figure 22 Illustration of Blue CL- GQDs #Glycine modified SPCE for electrochemical sensor application, show the current at potential 0.3 V	44
Figure 23 Illustration of Blue CL- GQDs #Glycine modified SPCE for electrochemical sensor application, show the current at potential -0.8 V	45
Figure 24 Illustration of Yellow CL- GQDs #Bicarbonate modified SPCE for electrochemical sensor application, Cyclic voltammograms of 5.0 mM $[\text{Fe}(\text{CN})_6]^{3-/4-}$ in 0.1 M KCl measured on different electrodes at a scan rate of 100 mVs^{-1} , and the corresponding peak current extracted from the CVs ($n=3$).	46
Figure 25 Illustration of Yellow CL- GQDs #Bicarbonate modified SPCE for electrochemical sensor application, , show the current at potential 0.3 V	46
Figure 26 Illustration of Yellow CL- GQDs #Bicarbonate modified SPCE for electrochemical sensor application, show the current at potential -0.8 V	47

CHAPTER I

INTRODUCTION

1.1 Introduction

In recent years, graphene quantum dots have seen extensive development, particularly in the realm of new synthesis due to their composition primarily consisting of carbon. They possess low toxicity, excellent biocompatibility with biological cells, high water solubility or dispersibility, ease of synthesis, high thermal stability, and conductivity. [1] Moreover, they exhibit fluorescence [2] and favorable electron transfer properties [3]. These properties make graphene quantum dots valuable in various technological and innovative fields, including sensors, drug delivery systems, bioimaging, and biosensors.

Graphene quantum dots (GQDs) were the first nanomaterials synthesized by Dengyu Pan et al. in 2010.[4] Using a hydrothermal process allows the transformation of graphene sheets from micrometer-sized graphene quantum dots to nanometer-sized graphene. These discovered graphene quantum dots are classified as carbon nanomaterials, with carbon as the primary structural component, forming a zero-dimensional system with diameters ranging from about 1 to 10 nanometers. However, in practical applications such as in sensor technology aimed at analyzing and detecting heavy metal materials using Screen-Printed Graphene Electrodes, larger particle sizes may be more appropriate, typically around 100 nanometers. This size is commonly utilized due to the advantages mentioned earlier. As a result of these properties, graphene quantum dots are intriguing nanomaterials that have expanded from a zero-dimensional (0-D) structure to become suitable for applications in innovation across various fields, transitioning from zero-dimensional (0-D) to one-dimensional (1-D), two-dimensional (2-D), and even three-dimensional (3-D) structures. [5].

My research aims to investigate the transformation of zero-dimensional (0-D) graphene quantum dots (GQDs) into structures suitable for electrochemical sensor applications. The focus is on effectively detecting metal ions by studying the temporal effects on the structural changes of graphene quantum dots.

The study examines how prolonged time intervals influence the electron concentration at the counter and working electrodes (applied potential -1.5 V), thereby causing transformations in the structure of graphene quantum dots. Analysis of the composition and characteristics of graphene quantum dots involves various analytical techniques, including Raman spectroscopy, scanning electron microscopy coupled with energy-dispersive X-ray spectroscopy (SEM-EDX), and transmission electron microscopy coupled with energy-dispersive X-ray analysis.

This research also aims to apply these graphene quantum dots in enhancing the electrochemical conductivity of graphene screen-printed electrodes for sensor applications. Cyclic voltammetry experiments will modify the working electrodes in the screen-printed electrode application. Screen-printed electrodes are generally designed to be small in size, making them user-friendly, cost-effective, and reducing the volume of chemicals used for analysis. Additionally, their disposable nature minimizes substance contamination.

1.2 Objectives of the Research

1. To study the effect of time of electrochemical reduction on the characteristics of GQDs prepared by electrochemical reduction on Ag electrodes.
2. To compare the performances of GQDs for using in Screen printed electrodes.

1.3 Scopes of the Research

1. Before the electrodeposition and electrolysis experiments, Cu foil (10×25mm²) were mechanically polished with 800G sandpaper and were rinsed with DI water before, then left to dry at room temperature.
2. The substrates used in this study were Cu foils.
3. The Ag electrocatalysts were prepared by electrodeposition of Ag on the substrate Cu foil at precursor concentrations of Ag 0.4 M. The current density for electrodeposition was set at 20 mA/cm². Pt rod was used as counter electrode. After the electrodeposition method, the catalysts were cleaned with deionized water several times before leaving them to dry at room temperature.
4. The Ag/Cu foil catalyst was dip in 50 mL GQDs (Blue CL- GQDs #Acetic, Blue CL- GQDs #Glycine and Yellow CL- GQDs #Bicarbonate) and 0.4 M (NH₄)₂SO₄,

transforming graphene quantum dot structure on Ag electrodes under electrochemical reduction at potential of -1.5 V vs. Ag/AgCl for different time was to set 15, 30, 45 and 60 min.

5. The catalysts were characterized by

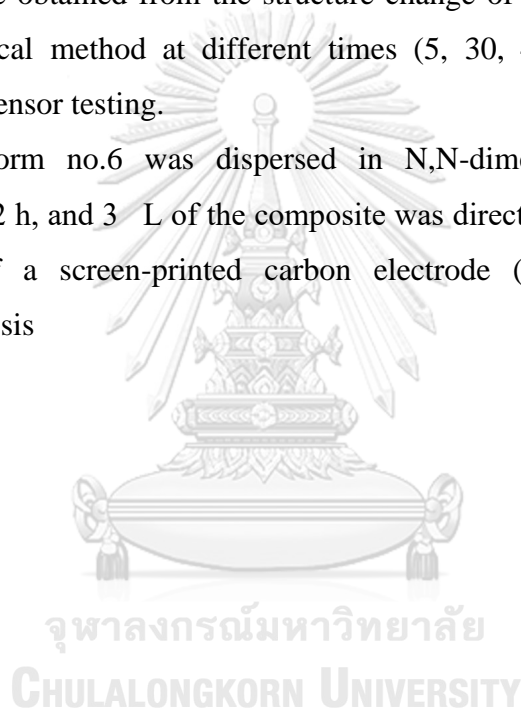
5.1. Scanning electron microscope-energy dispersive X-ray spectroscopy (SEM-EDX)

5.2. X-ray Photoelectron Spectroscopy (XPS)

5.3. Raman Spectroscopy

6. The sample obtained from the structure change of graphene quantum dots as well electrochemical method at different times (5, 30, 45 and 60 min.) were to Electrochemical Sensor testing.

7. Sample form no.6 was dispersed in N,N-dimethylformamide by using ultrasonicator for 2 h, and 3 L of the composite was directly dropped on the working electrode area of a screen-printed carbon electrode (SPCE), By using cyclic voltammetry analysis



CHAPTER II

BACKGROUND AND LITERAURE REVIEWS

2.1 Properties of graphene quantum dot

2.1.1 Physical Properties

Graphene quantum dots are classified as carbon nanomaterials primarily composed of carbon, featuring a zero-dimensional structure with a smaller diameter of 10 nanometers [6]. They typically exhibit a circular shape and comprise 1 to 10 graphene sheets. The in-plane lattice spacing of the graphite gap ranges from 0.18 to 0.24, while the graphitic inter-layer spacing measures 0.33 nm.

2.1.2 Electrochemical Properties

The electrochemical properties and electron transfer capability of graphene quantum dots depend on the arrangement of atoms. These quantum dots are small, typically less than 10 nm in diameter, providing a large surface area. Additionally, they possess a significant edge site area, facilitating efficient electron-molecule transfer. The majority of this transfer process occurs at the edges of the graphene quantum dots themselves [7]. Due to these advantages, graphene quantum dots are well-suited for sensor applications.

In graphene, the electrons in the 2s orbital and the electrons in the 2p orbital combine to form a hybrid orbital known as the sp² orbital. Figure 1 illustrates this electron configuration. The formation of the sp² electron binding results in the creation of a Sigma bond σ and three bonds in the 2p_x layer combined by covalent bonds, known as π bonds. Each carbon atom can undergo hybridization, forming energy bands of π and π^* . In hexagonal graphene structures, with three π -bonds bonded to carbon atoms, electrons are able to move freely (delocalized), allowing for various structural possibilities. This characteristic grants graphene excellent electrical properties [8].

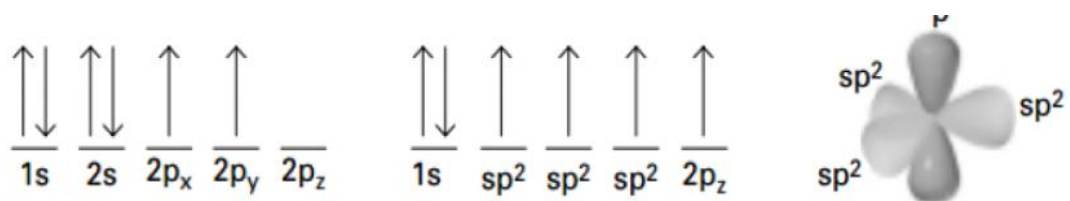


Figure 1 Electron arrangement of graphene

2.2 Electrodeposition of Ag electrocatalysts.

Electrodeposition or electroplating is a method used to coat a substrate with a metal through the electrochemical reduction of metal ions. The electroplating system comprises the object requiring coating (termed the cathode), an electrolyte, an anode, and a power source. The electrolyte's primary role is to provide conductivity, although certain electrolytes may have low conductivity. To address this issue, supporting electrolytes like salt, inorganic acids, and alkalis can be added. Importantly, these substances not only enhance conductivity but also reduce the required potential input.

2.3 Cyclic voltammetry (CV)

Cyclic voltammetry is a technique utilized in quantitative analysis, known for its simplicity and speed. The analysis reveals the correlation between the potential difference of the inserted electrode and the current, depicted in Figure 2. The current observed at the E_{pc} position arises from the reduction of the maximum cathode current. Both the peak current of the cathode and the current at the E_{pa} position are results of oxidation, identified as the Anode peak current. [9]

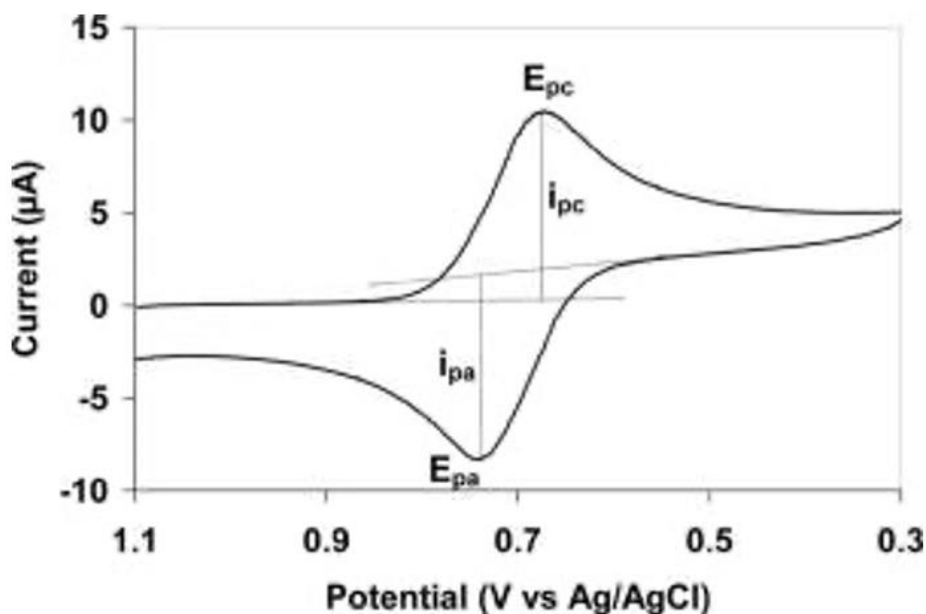


Figure 2 Cyclic voltammetry graph

2.4 Screen-printed electrodes (SPEs)

Screen-printed electrodes (SPEs) are electrochemical measurement devices created by printing various types of carbon on plastic or ceramic substrates. They enable rapid in-situ analysis with high reproducibility, sensitivity, and accuracy. The composition of different inks (carbon, silver, gold, platinum) used in manufacturing these electrodes dictates their selectivity and sensitivity. This flexibility allows analysts to design the most optimal device based on its intended purpose [10].

- Working electrode: Its response is sensitive to the analyte concentration.
- Reference electrode: It permits the application of a known potential independent of the analyte and other ion concentrations. Its potential remains constant, against which the potential of the working electrode is measured.
- Auxiliary or counter electrode: This electrode completes the circuit of the three-electrode cell, facilitating the flow of current. It enables the analysis of processes involving electronic transfer.

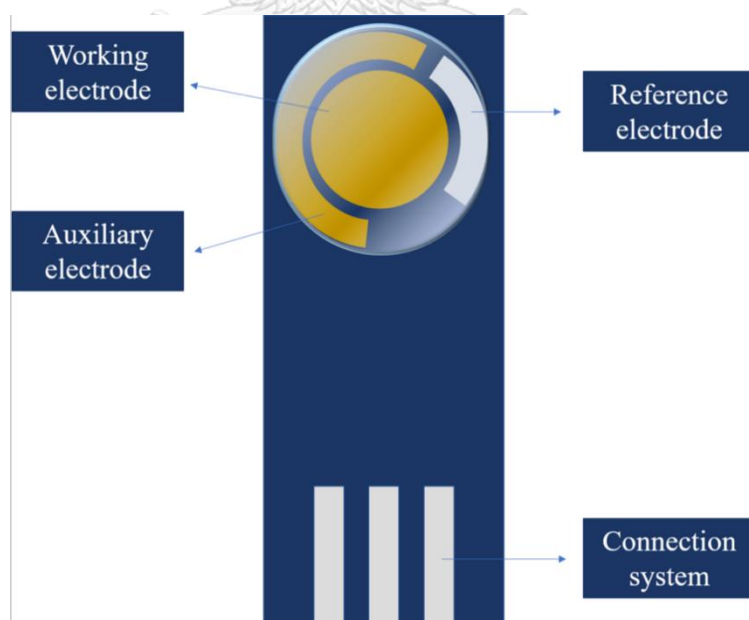


Figure 3 Screen-printed electrode with the three electrodes system

2.5 Fluorescent mechanism carbon dots

Carbon dots are nanoparticles exhibiting fascinating fluorescence properties, marked by their outstanding characteristics. Most carbon dots emit wavelengths where the intensity of fluorescence depends on the wavelength itself, offering versatile adjustments and modifications. Studies reveal that carbon dots fluoresce in the blue and green range (around 400 nanometers) and possess a potentially wide fluorescent span, extending to possibly 300-400 nanometers due to their nature. They can be derived from various raw materials through multiple processes, and their structure and surface properties are modifiable through various methods. This has spurred the study of carbon dots' optical properties to elucidate their fluorescent mechanisms. Consequently, it can be inferred that the fluorescence of carbon dots arises from the following mechanisms.

2.5.1 Quantum confinement

Quantum confinement is a phenomenon observed in nanometer-sized objects, allowing electrons to move freely within their wavelength range. Conductors smaller than 10 nanometers exhibit properties more akin to a semiconductor than a typical electrical conductor. Initially, when carbon dots were discovered, it was assumed that their luminescence resulted from quantum confinement due to their nanometer size and spherical or particle-like shape, resembling metal or metal nanoparticles, also known as quantum dots. The optical and electrical characteristics of quantum dots are influenced by this phenomenon, which relies on particle size. Smaller particles exhibit widened bandgaps, influencing their excitation wavelength and optical properties.

Hence, it's presumed that the fluorescence of carbon dots also arises from quantum confinement. Early studies revealed that the fluorescent properties of carbon dots are intricately tied to their precise size control. For instance, research on carbon dots synthesized from graphite via electrochemical methods demonstrated that dots sized at 1.2 nanometers emit light in the UV range at a 350-nanometer wavelength. Carbon dots ranging from 1.5 to 3 nanometers emit visible light between 400 and 700 nanometers, while those around 3.8 nanometers emit near-infrared light at 800 nanometers. This pattern suggests that as the size increases, the emitted wavelength lengthens or the bandgap narrows, aligning with the principles of quantum confinement.

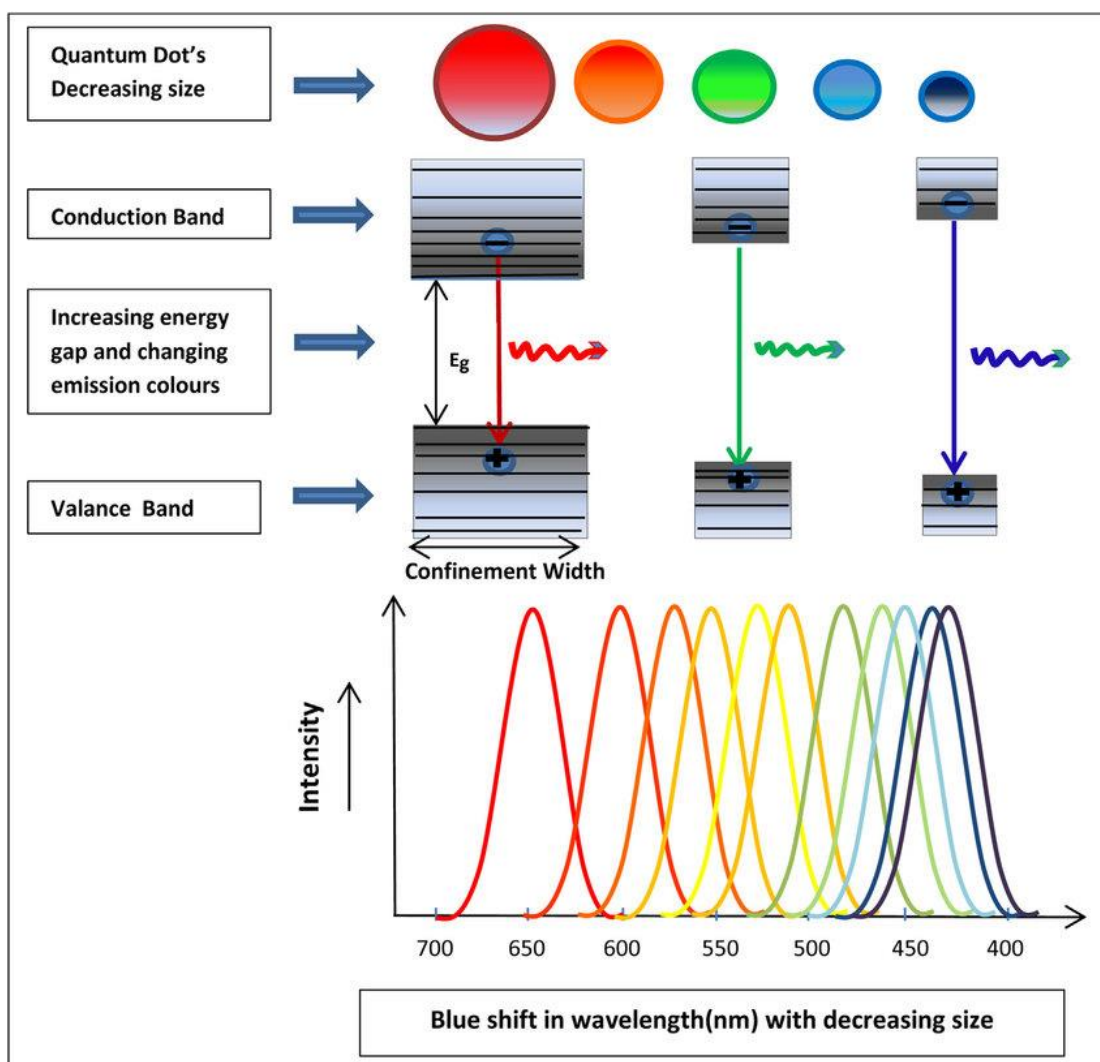


Figure 4 Illustration of quantum confinement effect.

Similar conclusions have been drawn from studies employing density functional theory (DFT) to investigate confinement in carbon dots. By computing the light wavelength of graphene fragments—termed graphene quantum dots—containing up to 170 carbon atoms, it was observed that the light wavelength transitions from UV to infrared as the size increases from 0.46 to 2.30 nm. This change results from the movement of pi electrons within the graphene quantum dot, indicative of the quantum confinement phenomenon. Furthermore, ultraviolet photoelectron spectroscopy (UPS) analysis revealed that smaller carbon dots exhibit reduced sp^2 or conjugate regions, leading to a wider bandgap. Conversely, larger carbon dots showed a shorter fluorescence lifetime, decreasing from 1.1 to 0.75 nanoseconds. Although larger carbon

dots enhanced electron mobility, energy was lost due to defect positions. Consequently, these studies underscore the significant influence of carbon dot size on their fluorescence.

2.6 Raman spectroscopy

Raman spectroscopy is a commonly employed technique to analyse the purity of graphene. Typically, carbon dots exhibit two prominent signals based on the C=C bond: the D-band and the G-band. The D-band, appearing at $1,350\text{ cm}^{-1}$, is caused by disordered Sp^2 carbon, while the G-band, observed at $1,600\text{ cm}^{-1}$, signifies the E-plane bonding of crystalline graphite carbon or ordered Sp^2 carbon. The ratio between the G-band and D-band indicates the quantity, crystallinity, and presence of carbon within the graphene quantum dot. In the spectral Raman analysis of graphene, the G-band holds particular significance.

2.7 Scanning electron microscope

The Scanning Electron Microscope (SEM) is an electron microscope that generates images by measuring electrons reflected from the surface of the surveyed sample, as depicted in Figure 5. The images produced by the SEM are three-dimensional, making them useful for studying the morphology and surface characteristics of the sample in detail. It is commonly utilized to examine the appearance of the sample's surface.

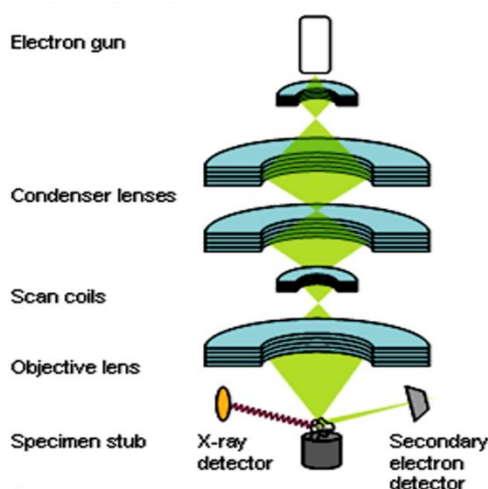


Figure 5 Analysis with a scanning electron microscope

The preparation of carbon dot samples for analysis with a scanning electron microscope typically involves distributing a powdered sample onto the platform and securing it using carbon tape. Subsequently, the sample is dried using a desiccator or silica gel before analysis. In general, images obtained using this method depict carbon dots as circular or oval-shaped entities. The size of carbon dots typically ranges from approximately 2 to 20 nanometers or even larger, depending on the substrate.

2.8 X-ray photoelectron spectroscopy

X-ray photoelectron spectroscopy is a widely-used technique for analyzing the elemental components of a sample and quantifying their proportions. This method relies on directing X-rays onto the sample. Samples intended for X-ray photoelectron spectroscopy need to be prepared as thin films. Samples deeper than 20 nanometers cannot be analyzed as electrons can't escape from depths beyond this threshold. Generally, two types of measurements are conducted: a survey scan and a high-resolution scan. The survey scan involves scanning over a broad energy range to provide an overall picture of the sample's elemental composition. It yields a spectrum indicating the binding energy and the quantity of released electrons from each element. Subsequently, a detailed scan of the element of interest is performed by selecting a narrow range of binding energy values. This focused scan is repeated several times to obtain a clear signal. This technique enables the analysis of the types and ratios of elements present in the sample.

CHAPTER III

MATERIALS AND METHODS

3.1 Materials

Table 1 Chemicals used as precursors and electrolyte.

Name	Formula	Suppliers
1. Ammonium Sulfate	$(\text{NH}_4)_2\text{SO}_4$	Thomas Baker
2. Silver Nitrate	AgNO_3	Sigma-Aldrich
3. Blue CL- GQDs #Acetic	GQDs # CH_3COOH	Crystallyte co., ltd.
4. Blue CL- GQDs #Glycine	GQDs # $\text{C}_2\text{H}_5\text{NO}_2$	Crystallyte co., ltd.
5. Yellow CL- GQDs #Bicarbonate	GQDs # HCO_3^-	Crystallyte co., ltd.

Table 2 Metals used as electrodes in electrodeposition method.

Electrodes	Suppliers
1. Copper foil (0.1 mm thick, 99.9999%)	Alfa Aesar
2. Platinum foil (0.1 mm thick, 99.9999%)	Alfa Aesar
3. Platinum rod (Length 76 mm, Diameter 2 mm)	Metrohm

3.2 Catalysts preparation

3.2.1 Preparation of electrodes

Cu foil ($10 \times 25 \text{ mm}^2$) as shown in Table 2. were mechanically polished with 800 G sandpaper and were cleaned with DI water. Then, the polished electrodes were dried at room temperature.

3.2.2 Preparation of Ag catalysts (Ag/Cu)

Ag catalysts were deposited on Cu foil ($10 \times 10 \text{ mm}^2$) in 0.01 M AgNO_3 and 0.6 M $(\text{NH}_4)_2\text{SO}_4$, used as a supporting electrolyte, as shown in Table 1. to increase ionic

strength solutions via the electrodeposition method. These electrodes were performed in a two-electrode system containing Pt rod used as an anode, and the electrode, which was Cu foil, used a cathode. The current density was fixed at 20 mA/cm^2 for 20 s. during synthesis catalysts. When the electrodeposition process was finished, the Ag catalysts were washed with DI water before left them dried at room temperature.

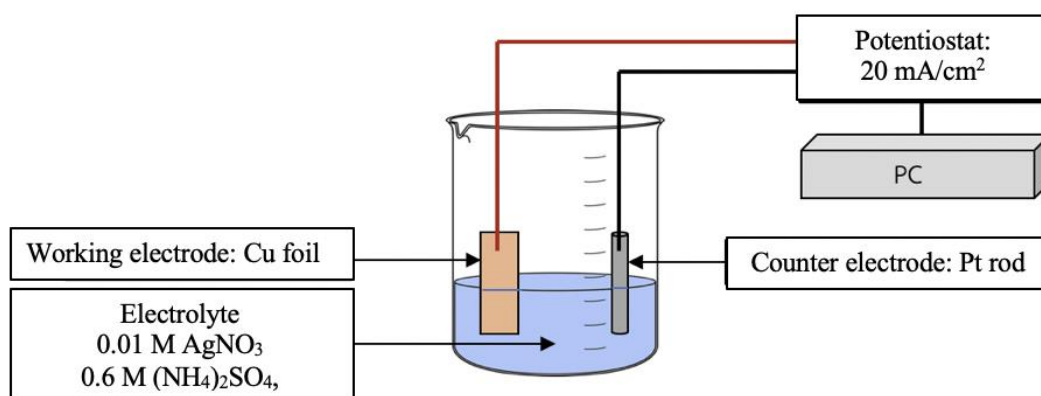


Figure 6 Schematic of electrodeposition of Ag catalysts on different substrates.

3.3 Electrochemical transformation structure experiment of graphene quantum dots

The Ag/Cu foil catalyst was dip in 50 ml GQDs (Blue CL- GQDs #Acetic, Blue CL- GQDs #Glycine and Yellow CL- GQDs #Bicarbonate) as shown in Table 1, which was used as the electrolyte. Position the electrode as in Figure 7 with Pt foil used as the anode. The Ag/Cu foil used as the cathode and the reference electrode (Ag/AgCl) is the potential electrode. Then a constant current of -1.5 V was applied at different time was to set 15, 30, 45 and 60 min. When the electrodeposition process was finished, the Ag/Cu foil were washed with DI water before left them dried at room temperature. The copper foil was scraped to analyze the composition and structure of the graphene quantum dots.

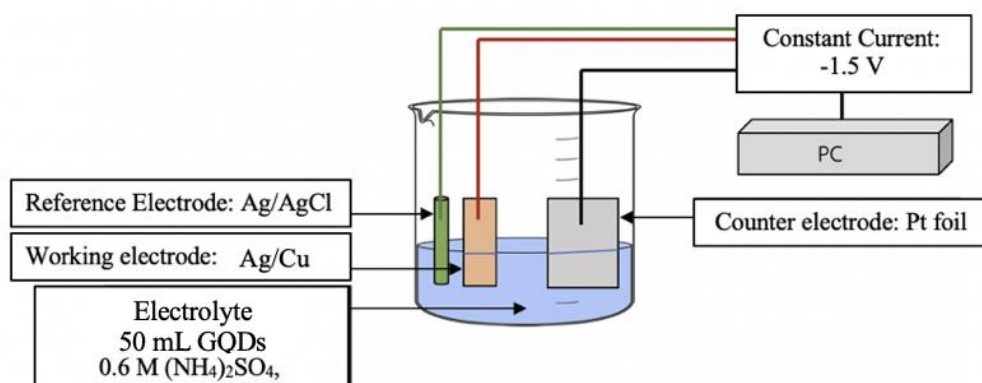


Figure 7 Electrode positioning for electrochemical deformation experiment of graphene quantum dots.

3.4 Characterization

3.3.1 Scanning electron microscope-energy dispersive X-ray spectroscopy (SEM-EDX)

The sample obtained from the structure change of graphene quantum dots as well electrochemical method at different times (5, 30, 45 and 60 min.) were characterized by scanning electron microscopy (SEM) of Hitachi mode S-3400N and energy dispersive X-ray spectroscopy (EDX) to investigate the morphology of the surface and the bulk composition, respectively.

3.3.2 X-ray Photoelectron Spectroscopy (XPS)

The sample obtained from the structure change of graphene quantum dots as well electrochemical method at different times (5, 30, 45 and 60 min.) were characterized by The XPS spectra were obtained using the Amicus spectrometer (Kratos, Manchester, UK) with Mg $K\alpha$ X-ray gun at accelerating voltage 10 kV and current of 20 mA. The elemental binding energy (Cu, O, N, Ag, C and S) was used to analyzing the elements that are the components of a sample and measuring their quantities.

3.3.3 Raman Spectroscopy

The sample obtained from the structure change of graphene quantum dots as well electrochemical method at different times (5, 30, 45 and 60 min.) were characterized by Raman Spectroscopy of Waltham, USA at laser light source with a

wavelength of 532 nm and a laser output of 10 mW was used to investigate the molecular structure.

3.5 Electrochemical Sensor

The sample obtained from the structure change of graphene quantum dots as well electrochemical method at different times (5, 30, 45 and 60 min.) were dispersed 2 mg of the substance in 1 mL of DMF, then sonicated for 3 hr. Then drop 1 uL of the substance onto the face of the working electrode, let it dry at room temperature, then drop.1 uL of the substance was applied to the electrode surface again and allowed to dry at room temperature. Cyclic voltammograms of 5.0 mM $[\text{Fe}(\text{CN})_6]^{3-/4-}$ in 0.1 M KCl measured on different electrodes at a scan rate of 100 mVs^{-1} , and the corresponding peak current extracted from the CVs ($n=3$).

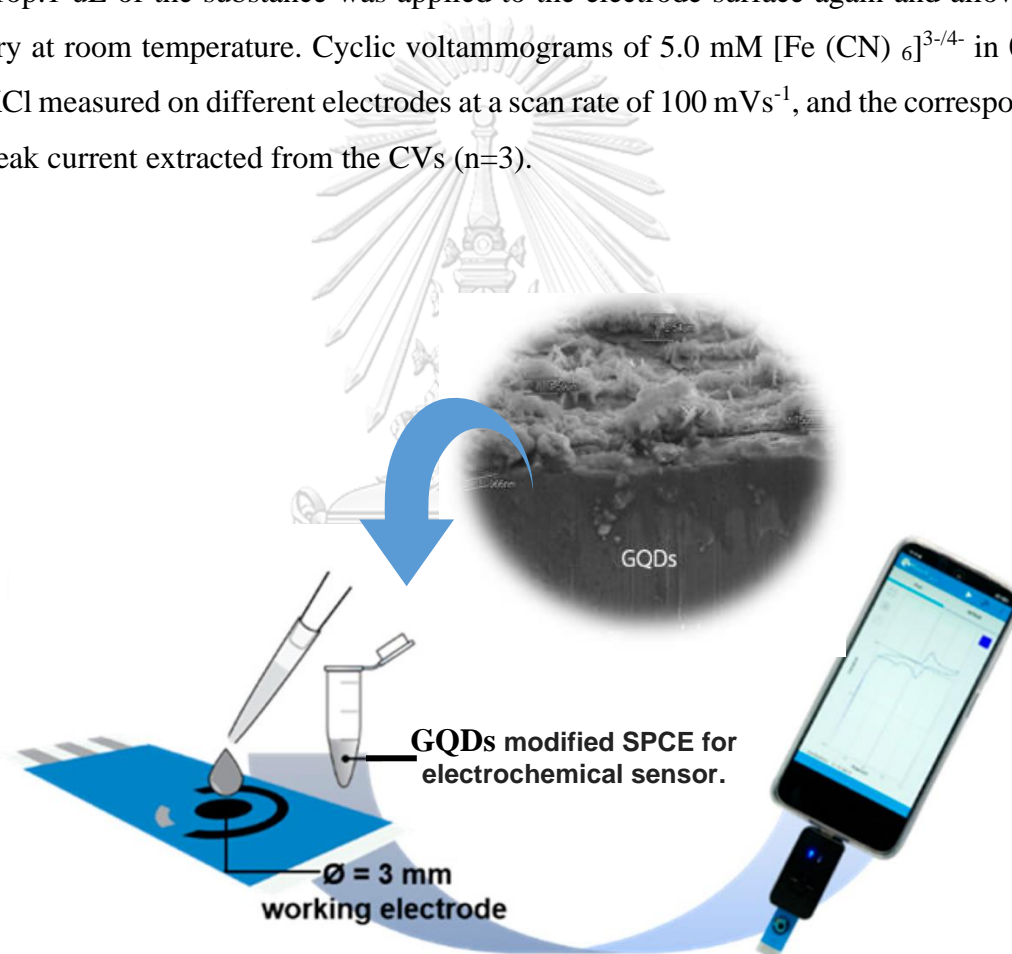
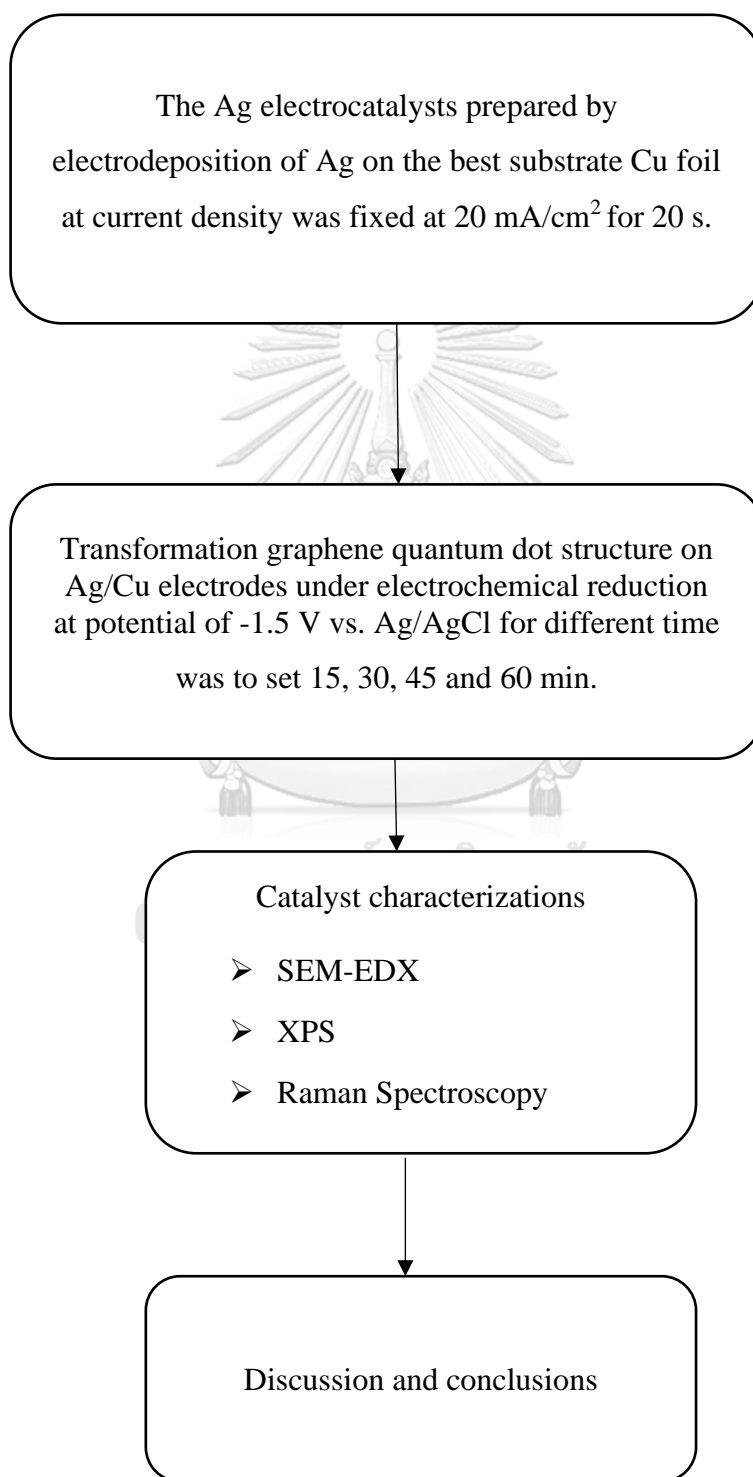


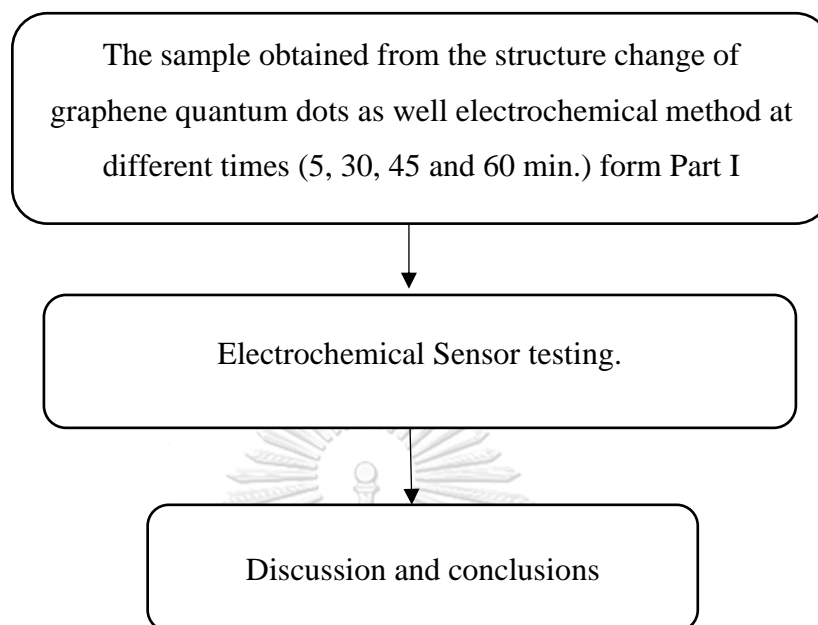
Figure 8 Electrochemical Sensor testing.

3.6 Research methodology

Part I. To study the effect of time of electrochemical reduction on the characteristics of GQDs prepared by electrochemical reduction on Ag electrodes.



Part II. To compare the performances of GQDs for using in Screen printed electrodes



For reporting the results, define the code in various conditions as follows:

Table 3 Code for calling the sample in each condition.

Code	GQDs	Reaction Times (min.)
1. B-A-15	Blue CL- GQDs #Acetic	15
2. B-A-30	Blue CL- GQDs #Acetic	30
3. B-A-45	Blue CL- GQDs #Acetic	45
4. B-A-60	Blue CL- GQDs #Acetic	60
5. B-G-15	Blue CL- GQDs #Glycine	15
6. B-G-30	Blue CL- GQDs #Glycine	30
7. B-G-45	Blue CL- GQDs #Glycine	45
8. B-G-60	Blue CL- GQDs #Glycine	60
9. Y-B-15	Yellow CL- GQDs #Bicarbonate	15
10. Y-B-30	Yellow CL- GQDs #Bicarbonate	30
11. Y-B-45	Yellow CL- GQDs #Bicarbonate	45
12. Y-B-60	Yellow CL- GQDs #Bicarbonate	60

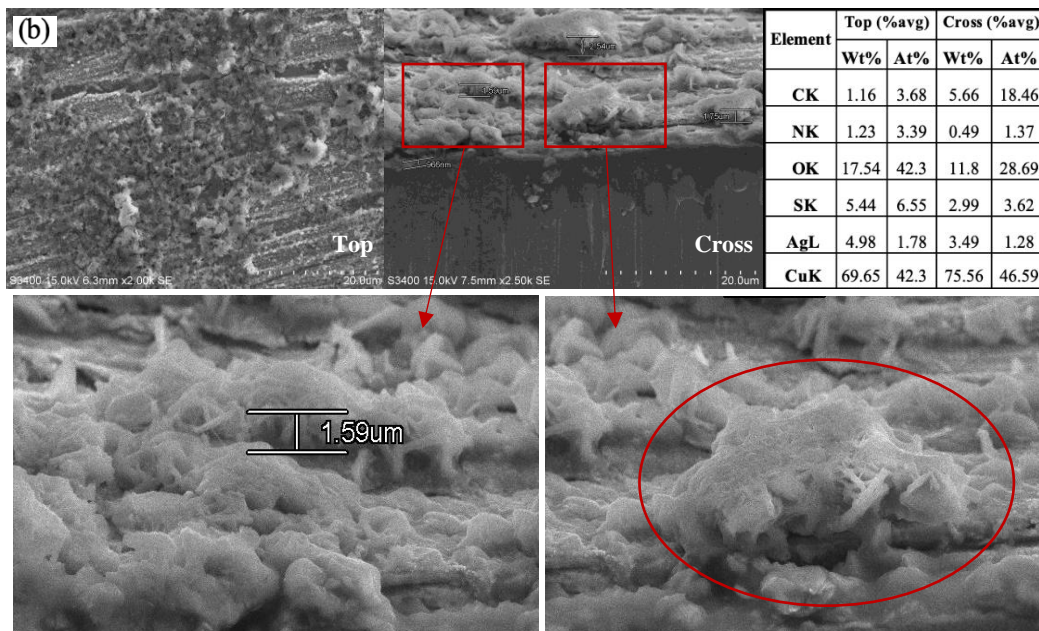
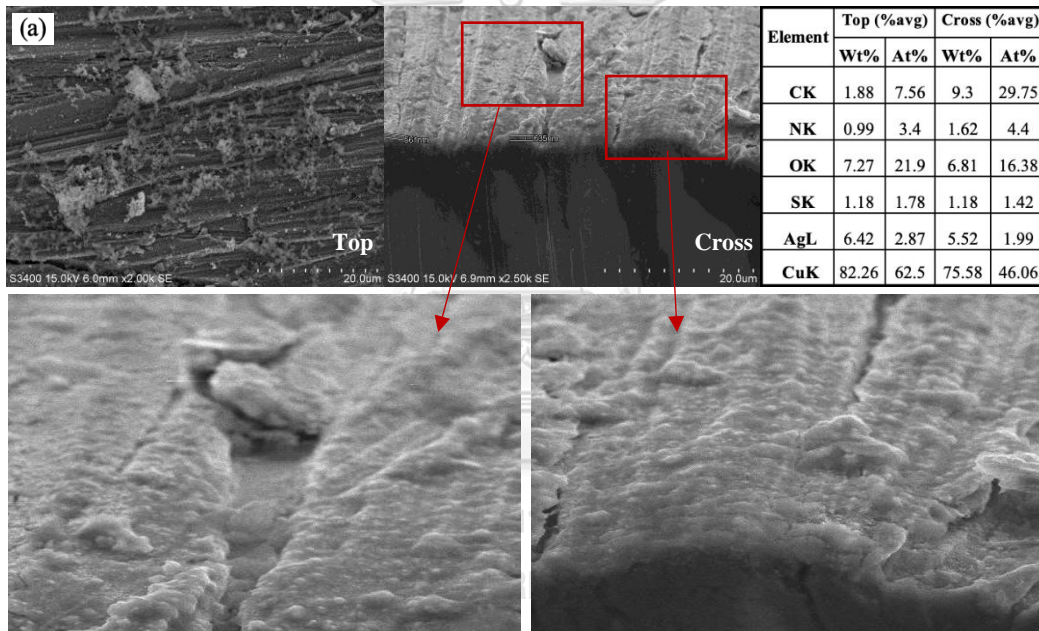
CHAPTER IV

RESULTS AND DISCUSSION

Part I. To study the characteristics of the GQDs performances of Ag electrodes different time (15,30,45,60 minutes).

4.1 Characterization of the sample by Scanning electron microscope-energy dispersive X-ray spectroscopy (SEM-EDX)

4.1.1 Scanning electron microscope-energy dispersive X-ray spectroscopy (SEM-EDX) of Blue CL- GQDs #Acetic different times (15, 30, 45 and 60 min.)



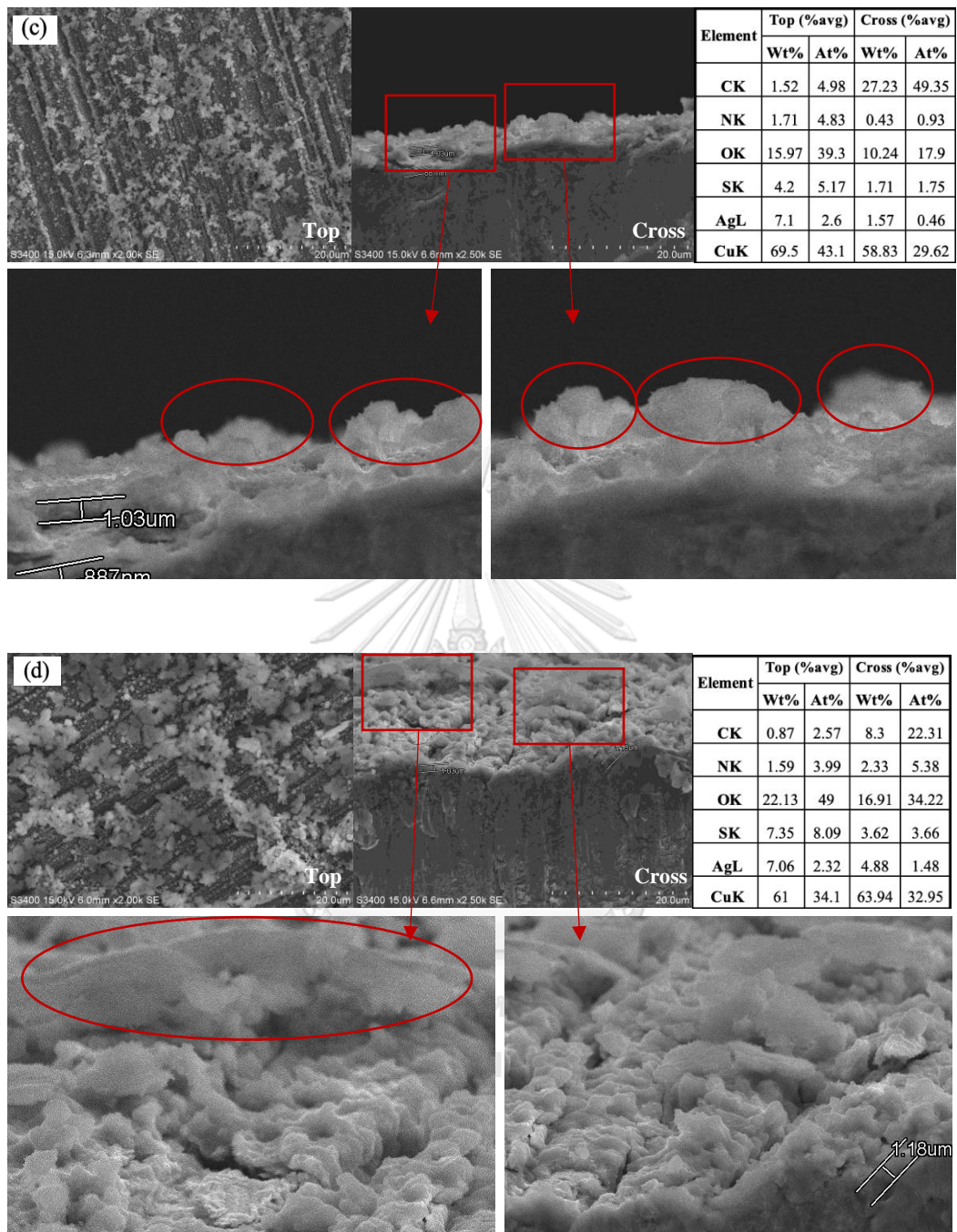


Figure 9 SEM-EDX images of Blue CL-GQDs #Acetic different times:
 (a) 15 minutes (b) 30 minutes (c) 45 minutes (d) 60 minutes

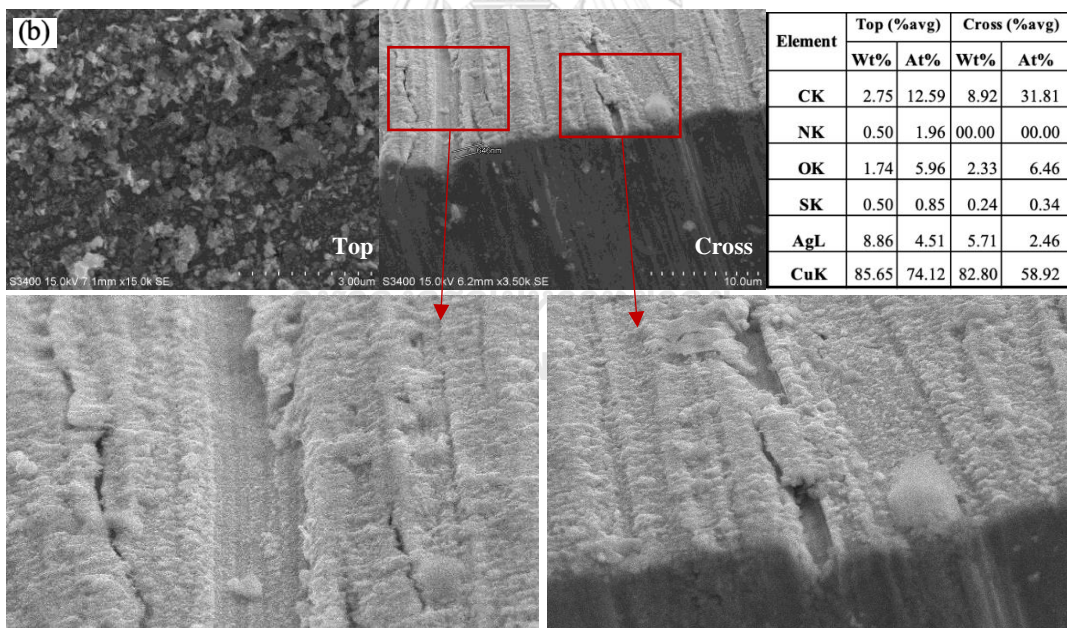
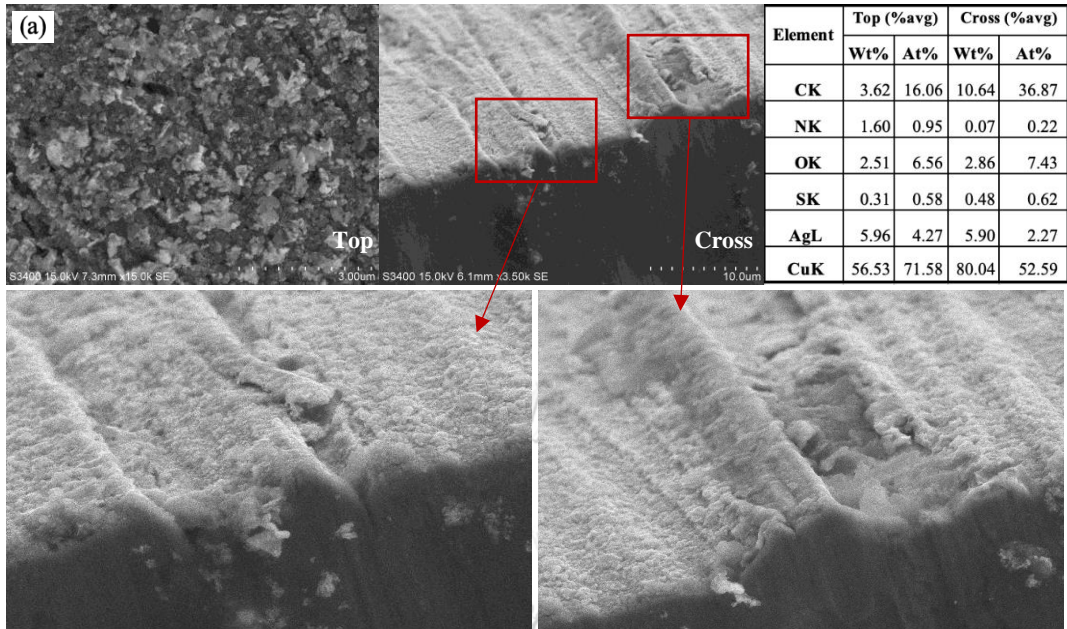
Table 4 Table for comparison all of condition Carbon (C) percent by atom and particle size of Blue CL- GQDs #Acetic.

Sample	CK (At% avg)		Particle thickness(um)	Morphology
	Top	Cross		
B-A-15	7.56	29.75	0.56 – 0.64	Smooth thin films
B-A-30	3.68	18.46	1.59 - 2.54	3D structure
B-A-45	4.98	49.35	0.97-1.03	3D structure and Smooth thin films
B-A-60	2.57	22.31	1.03-1.08	Smooth thin films

The obtained carbon through electrochemical reduction at different times was investigated to understand how substrates affect the morphologies of the prepared electrocatalysts. Figure 9 shows the SEM images of Blue CL-GQDs #Acetic at different times: 15, 30, 45, and 60 minutes, respectively. The electrocatalysts displayed similar dendrite-like structures. These results indicate that time slightly influences the morphology of GQDs. However, the particle size of B-A-30, B-A-45, and B-A-60 at 30, 45, and 60 minutes respectively, exhibited significantly smaller sizes when compared to the particle size of dendrites of B-A-15 at 15 minutes. Specifically, it was observed that the particle sizes of B-A-15, around 561nm-635nm, were larger than those of (B-A-30, B-A-45, and B-A-60), around 1.03-1.75 nm. This suggests that the particle sizes depended on the operation time, with fewer operating times resulting in larger particle sizes. Furthermore, it is suggested that the morphologies of GQDs (such as shape and particle size) are influenced by the duration of time. The table in Figure 9 illustrates the percentage of carbon atoms operated during each time. It was observed that the greatest number of carbon atoms was 18.46 At% for B-A-30, followed by 7.56 At% for B-A-15, 4.98 At% for B-A-45, and 2.57 At% for B-A-60, respectively.

Typically, the deposition of silver results in a dendrite-like structure that fills the silver area, leading to a substantial accumulation of electrons and high energy transformation of the GQDs. In the case of sample B-A-15 at 15 minutes, the GQDs have just begun accumulating and still retain their deformation energy. Each structure undergoes slight changes, giving the appearance of smooth thin films. For samples B-A-30 and B-A-45, after reactions lasting 30 and 45 minutes respectively, the structure of the GQDs begins to transition into a 3D structure. However, in the case of sample B-A-60 after a 60-minute reaction, it was observed to be covered with a carbon layer, reducing the electric field's energy and causing the structure to revert to its initial smooth thin film appearance, akin to that of B-A-15.

4.1.2 Scanning electron microscope-energy dispersive X-ray spectroscopy (SEM-EDX) of Blue CL- GQDs #Glycine different times (5, 30, 45 and 60 min.)



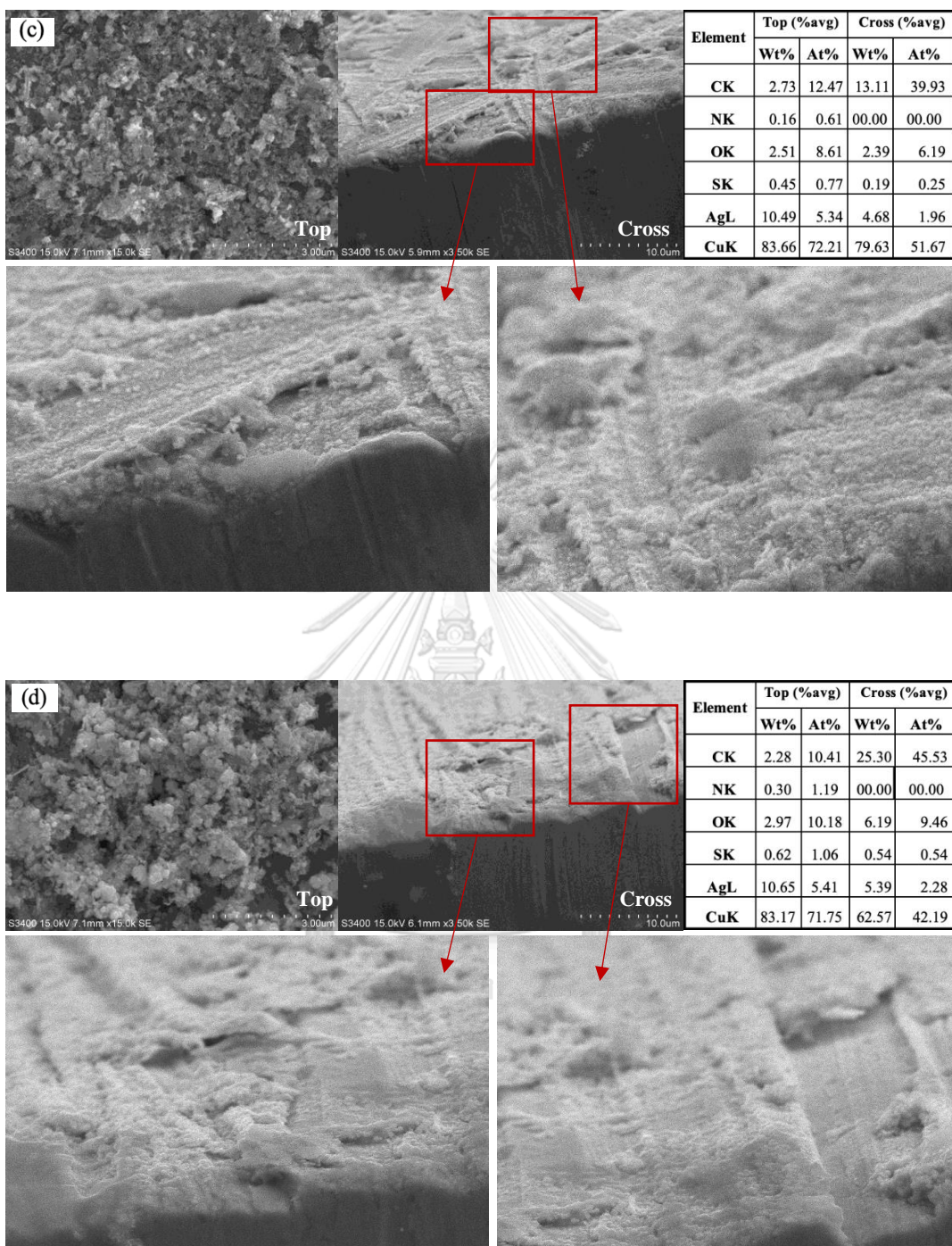


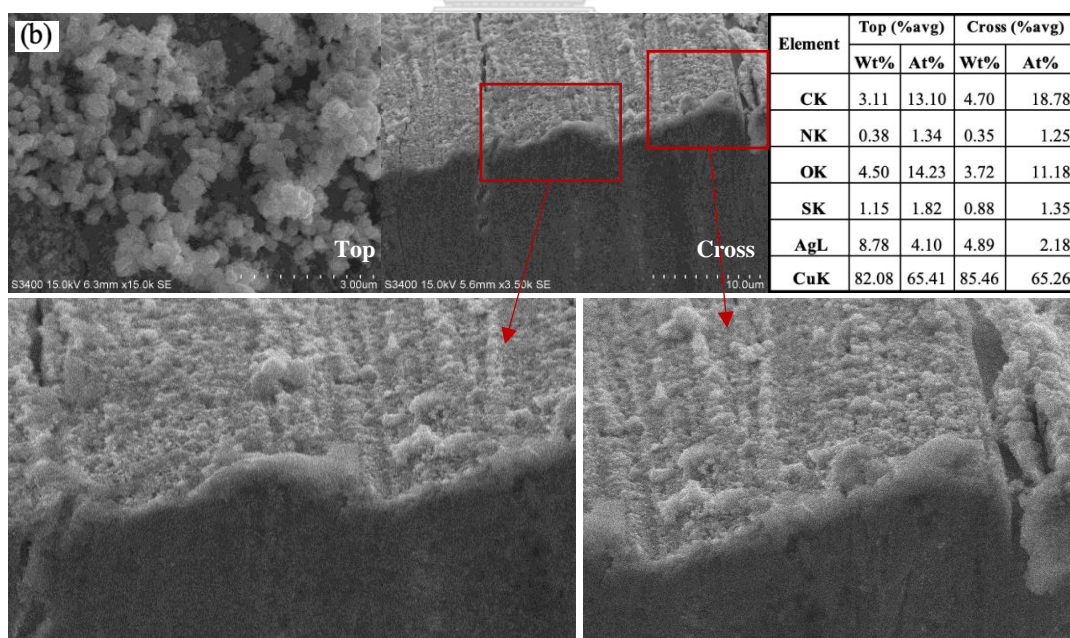
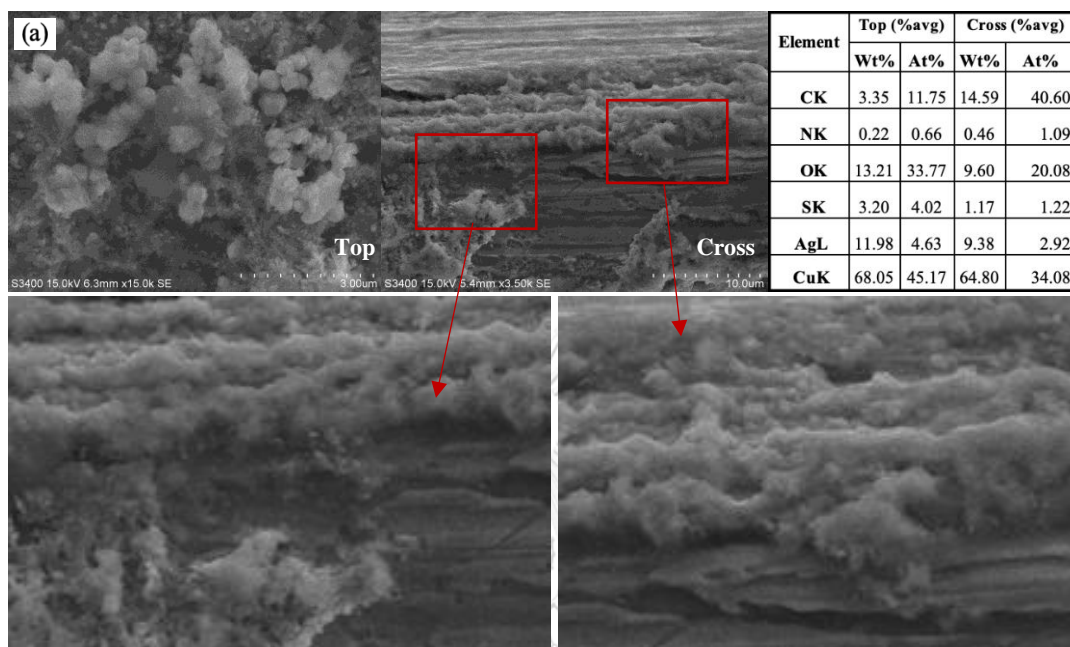
Figure 10 SEM-EDX images of Blue CL- GQDs #Glycine different times: (a) 15 minutes (b) 30 minutes (c) 45 minutes (d) 60 minutes

Table 5 Table for comparison all of condition Carbon (C) percent by atom and particle size of Blue CL- GQDs # Glycine.

Sample	CK (At% avg)		Particle thickness (um)	Morphology
	Top	Cross		
B-G-15	16.06	36.87	0.634	smooth thin film
B-G-30	12.59	31.81	0.646	smooth thin film
B-G-45	12.47	39.93	0.626	smooth thin film
B-G-60	10.41	45.53	0.907	smooth thin film

The carbon obtained from Blue CL-GQDs #Glycine at different times (15, 30, 45, and 60 min) is depicted in Figure 10, showcasing SEM images. The morphology of B-G-15 at 15 minutes appears as a smooth thin film, with an atomic weight from the top view measuring around 16.06 At%. In the image at 30 minutes, the morphology shows a structure quite similar to the GQDs observed at 15 minutes, with nearly identical surface features resembling a smooth thin film. The atomic weight at 30 minutes slightly decreases to 12.59% At. The SEM results of Blue CL-GQDs at 45 minutes reveal a morphology akin to that observed at 15 and 30 minutes, displaying some spots indicating a 3D structure, yet the majority of the surface still presents as a smooth thin film. The atomic weight registers around 12.47%. Regarding the CL-GQDs at 60 minutes observed via SEM, the morphology appears quite similar to the ones observed at 15, 30, and 45 minutes, with the surface maintaining the appearance of a smooth thin film. The atomic weight is at its lowest, measuring around 10.41%.

4.1.3 Scanning electron microscope-energy dispersive X-ray spectroscopy (SEM-EDX) of Yellow CL- GQDs #Bicarbonate different times (5, 30, 45 and 60 min.)



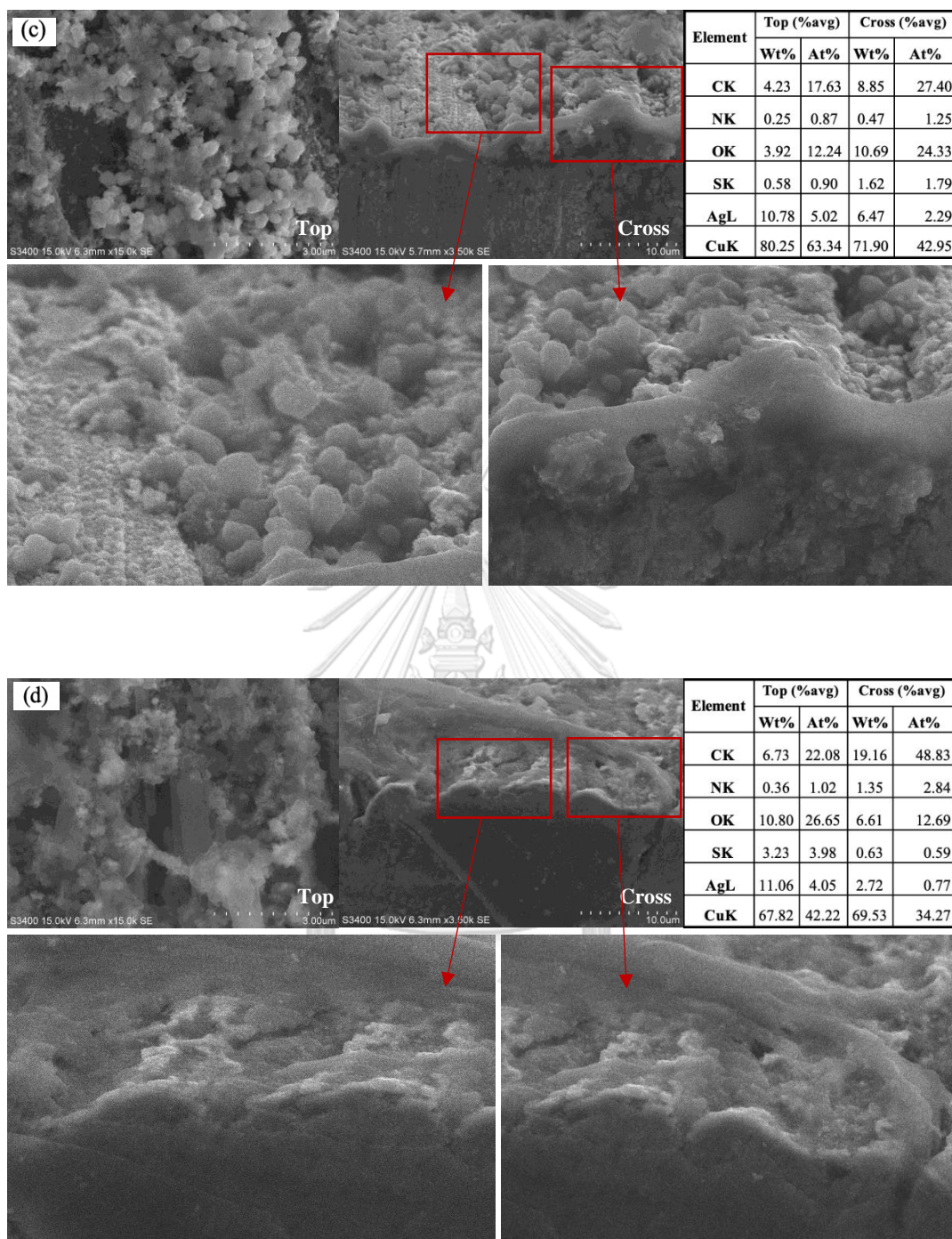


Figure 11 SEM-EDX images of Yellow CL- GQDs #Bicarbonate different times: (a) 15 minutes (b) 30 minutes (c) 45 minutes (d) 60 minutes

Table 6 Table for comparison all of condition Carbon (C) percent by atom and particle size of Blue CL- GQDs # Glycine.

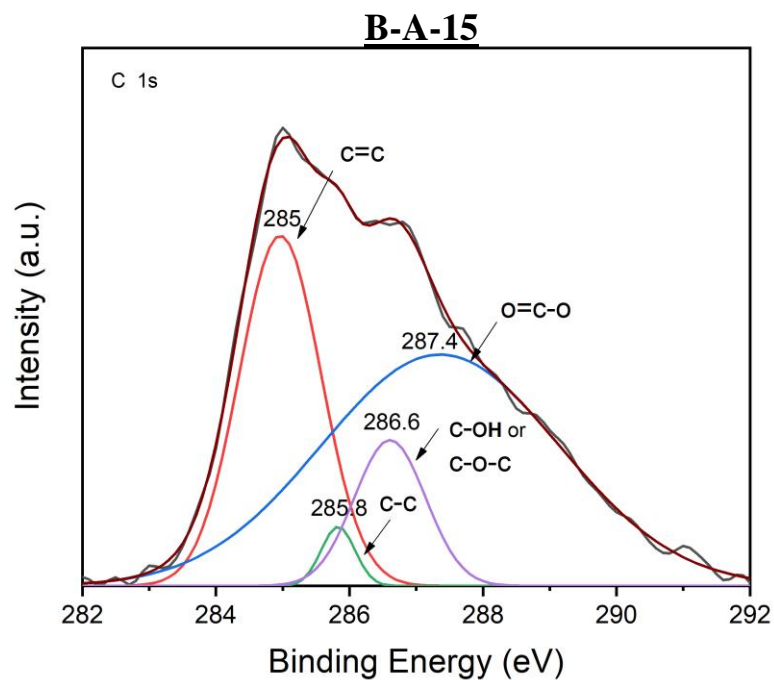
Sample	CK (At% avg)		Particle thickness (um)	Morphology
	Top	Cross		
Y-B-15	11.75	40.60	0.680	3D structure
Y-B-30	13.10	18.78	0.567	3D structure and Smooth thin films
Y-B-45	17.63	27.40	0.794	3D structure
Y-B-60	22.08	48.83	0.680	3D structure

The SEM images depict Yellow CL-GQDs #Bicarbonate at different times: 15, 30, 45, and 60, respectively. The electrocatalysts exhibit similar dendrite morphology across these durations. These results indicate that time influences the morphology of GQDs, as they start transitioning into a 3D structure due to the accumulation of electrons, resulting in high energy transformation.

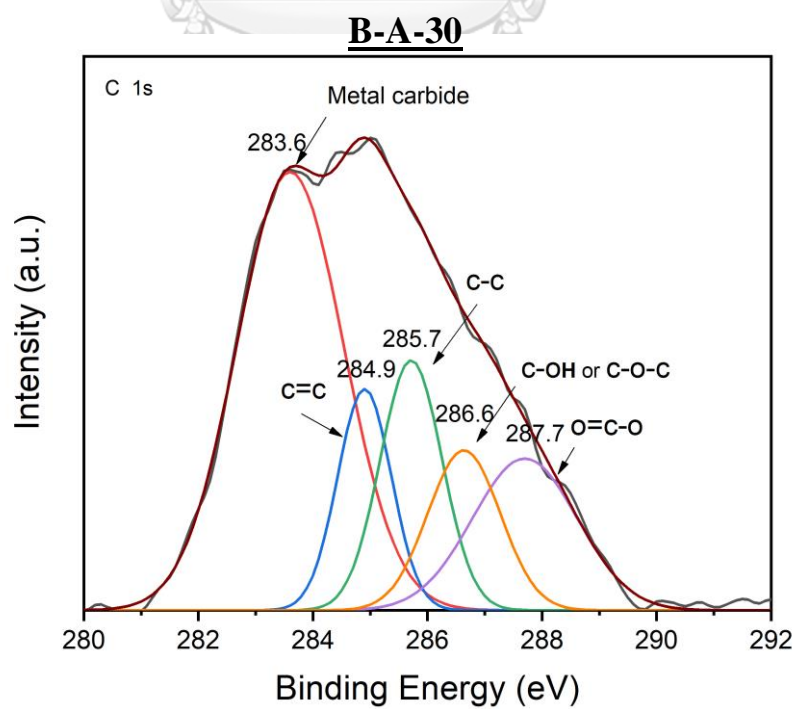
However, for GQDs observed at 45 and 60 minutes, some spots with smooth thin film cover on the 3D structure are noted. This change is influenced by the increased time, leading to a decrease in the electric field's energy, causing the structure to revert to its smooth thin film state covered with carbon layers. It was observed that the greatest number of carbon atoms were at 11.75 At% for Y-B-15, followed by 13.10 At% for Y-B-30, 17.63 At% for Y-B-45, and 22.08 At% for Y-B-60, respectively. The atomic weight increases with an increase in reaction time.

4.2 Characterization of the sample by X-ray Photoelectron Spectroscopy (XPS)

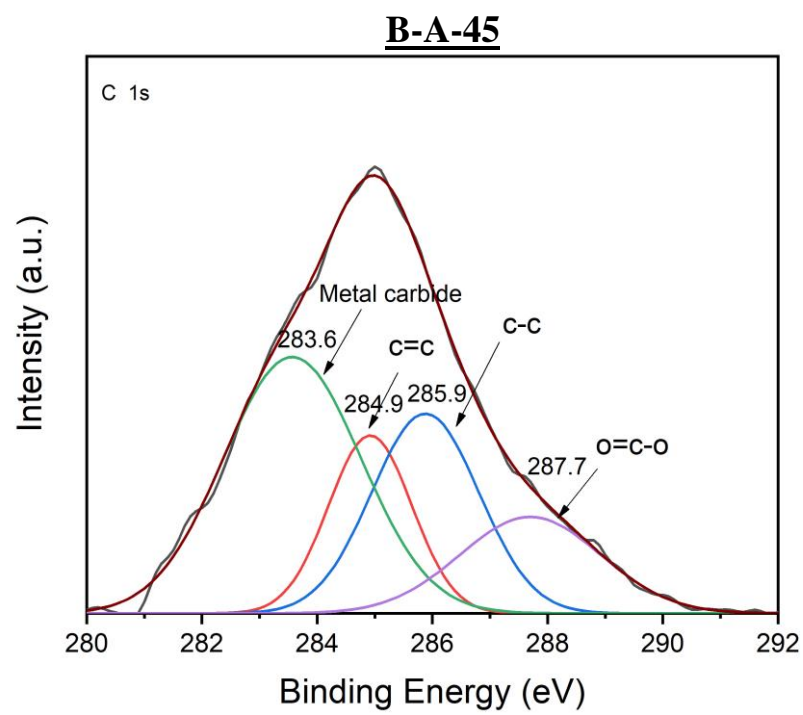
4.2.1 X-ray Photoelectron Spectroscopy of Blue CL- GQDs #Acetic different times (5, 30, 45 and 60 min.)



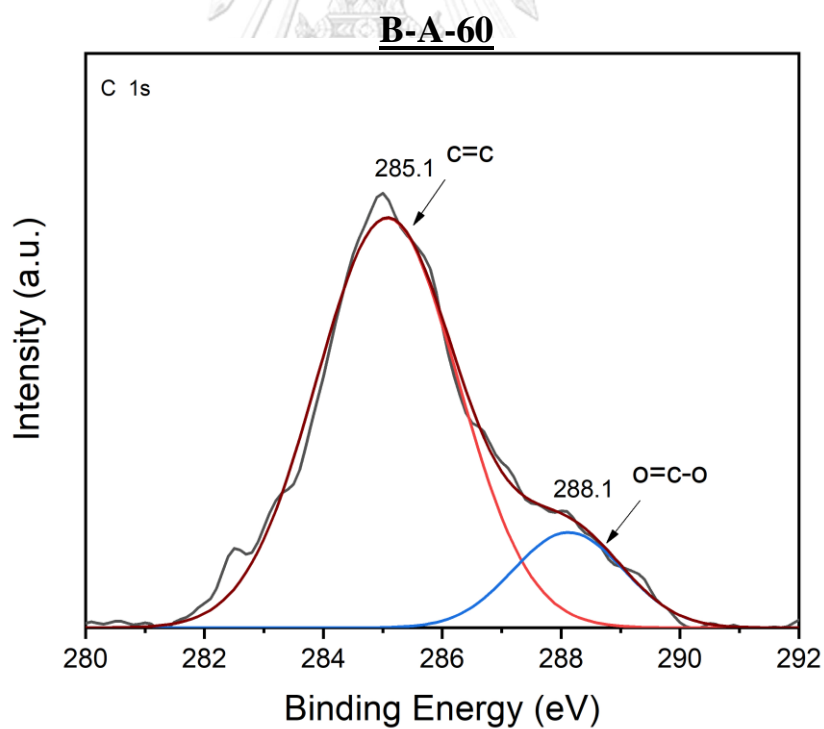
(a)



(b)



(c)



(d)

Figure 12 XPS image of Blue CL- GQDs #Acetic different times:
(a) 15 minutes (b) 30 minutes (c) 45 minutes (d) 60 minutes

Table 7 Contribution of carbon states to the total C 1s spectrum (%) in transformation Blue CL- GQDs #Acetic structure on Ag electrodes under electrochemical reduction.

Sample	%sp ²	%sp ³	% Oxygenic functional group	sp ³ to sp ² ratio
B-A-15	29.80	2.07	68.13	0.07
B-A-30	11.70	15.19	27.06	1.30
B-A-45	17.43	25.18	16.02	1.44
B-A-60	84.58	-	15.42	-

At B-A-15 with a reaction time of 15 minutes, Figure 12 (a) shows XPS spectra demonstrating C=C, C-C, C-OH, or C-O-C, and O=C-O species detected at 285.0, 285.8, 286.6, and 287.4 eV, respectively. The Sp³ to sp² ratio and the percentage of carbon species bonded to oxygen atoms in supra carbon dots, following a 15-minute reaction, were calculated to be 0.07 and 68.1%, as shown in Table 7.

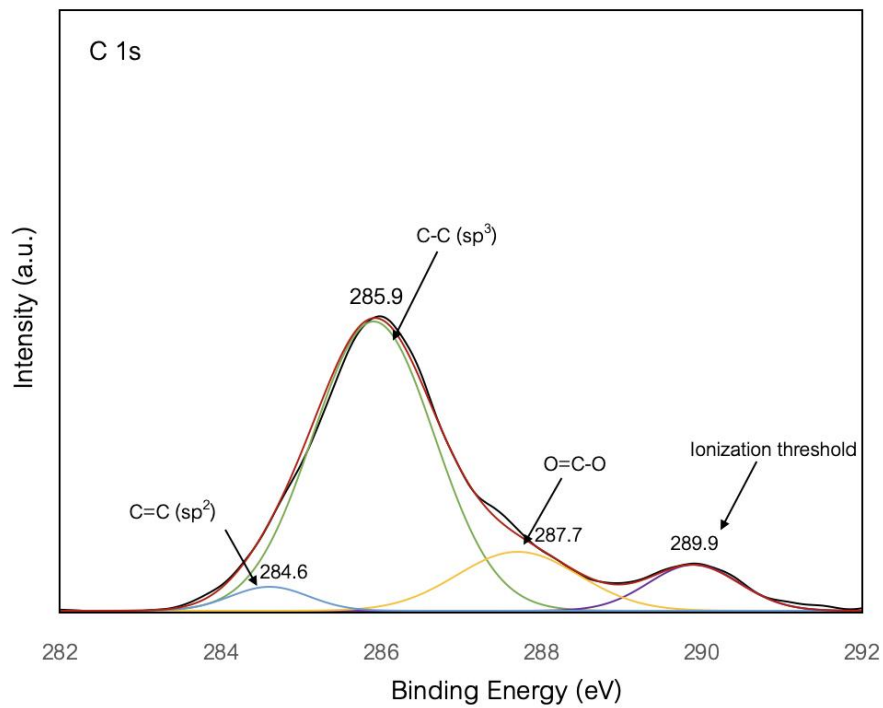
After an additional 15 minutes of processing, observations still revealed the presence of C=C, C-C, C-OH or C-O-C, and O=C-O species detected at 284.9, 285.7, 286.6, and 287.7 eV, respectively. A new peak at 283.6 eV emerged in Figure 12 (b), attributed to the presence of metal carbide species. The Sp³ to sp² ratio increased almost twentyfold from 0.07 to 1.30, as indicated in Table 7. Additionally, there was a significant drop in the percentage of carbon species bonded to oxygen atoms, decreasing from 68.1 to 27.1%, as shown in Table 4. The presence of metal carbides suggests that the formation of supra carbon dots proceeded through Ag NPs (nanoparticles) electrocatalysts, deoxygenating the oxygenic functional groups and subsequently forming sp³ C-C bonds.

In the case of sample B-A-45, where the reaction time was extended to 45 minutes, the observed carbon species in the XPS spectra remain consistent with those of B-A-30 at 30 minutes, albeit with a slight shift in location. Metal carbides, C=C, C-C, and O=C-O species were detected at 283.6, 284.9, 285.9, and 287.7 eV, as shown in Figure 12 (c), accompanied by the absence of C-OH or C-O-C species. There was an additional reduction in the percentage of carbon species bonded to oxygen atoms, decreasing from 27.1 to 16%, as indicated in Table 4. Simultaneously, there was a slight increase in the sp³ to sp² ratio from 1.30 to 1.44, suggesting further deoxygenation and transform processes resulting from the extended reaction time.

Due to the substantial accumulation of supra carbon dots on the cathode, impeding contact between the subsequent GQDs and Ag NP electrocatalyst, the transformation of GQDs into supra carbon dots is hindered. In the case of sample B-A-60 processed for 60 minutes, the layer of supra carbon dots entirely inhibits the transformation process. Consequently, there is no transformation observed on the outermost layer; instead, there is agglomeration of GQDs on this layer. This results in XPS spectra exhibiting only C=C and O=C-O species, observed at 285.1 and 288.1 eV, as shown in Figure 12 (d).

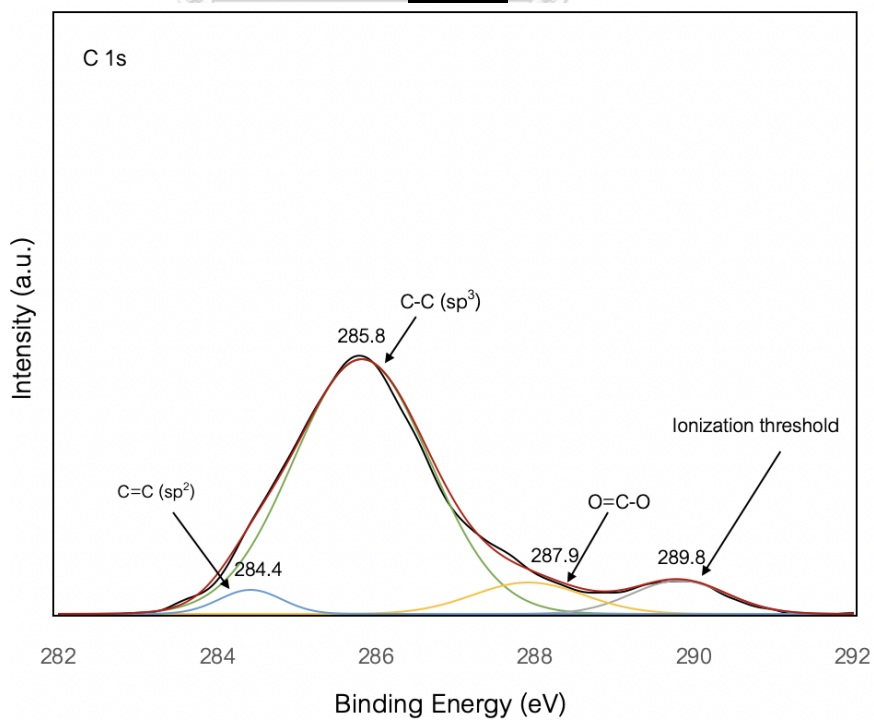
4.2.2 X-ray Photoelectron Spectroscopy of Blue CL- GQDs #Glycine different times (5, 30, 45 and 60 min.)

B-G-15

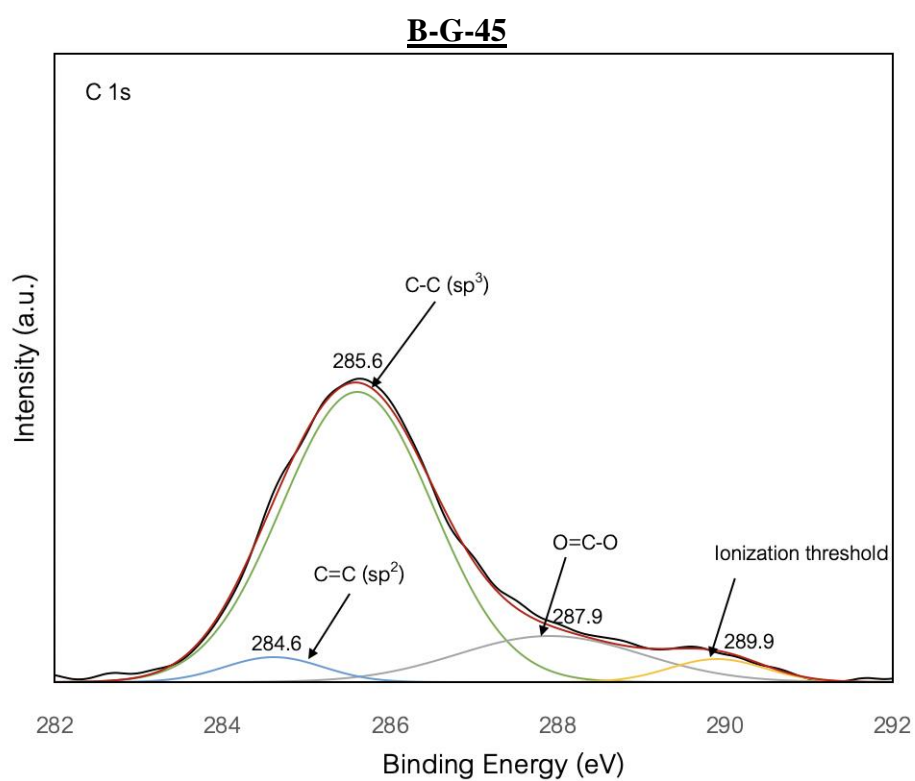


(a)

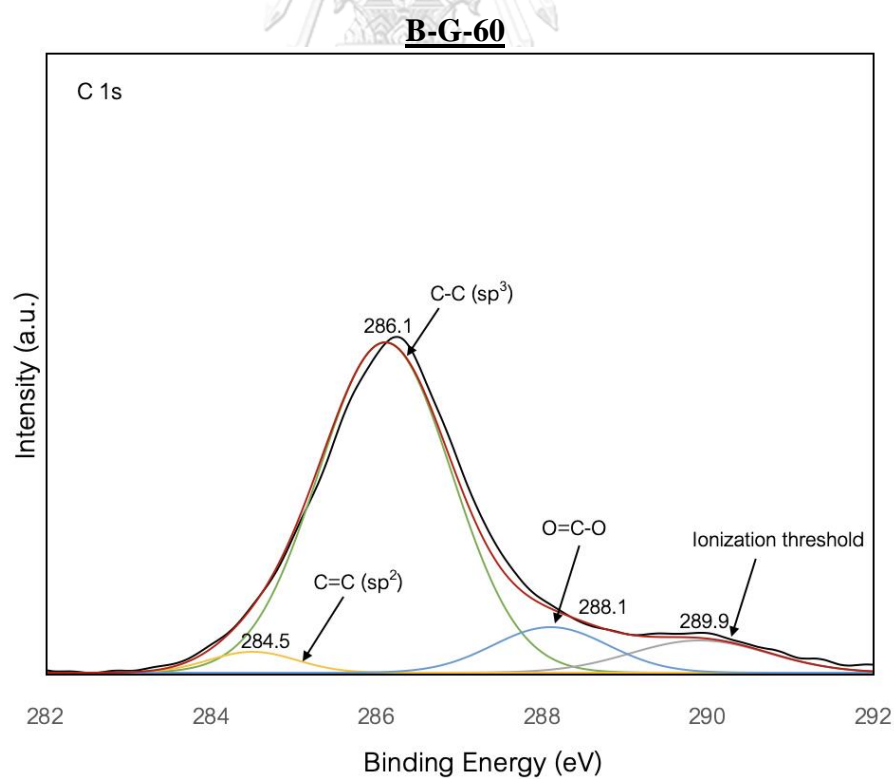
B-G-30



(b)



(c)



(d)

Figure 13 XPS image of Blue CL- GQDs #Glycine different times:
(a) 15 minutes (b) 30 minutes (c) 45 minutes (d) 60 minutes

Table 8 Contribution of carbon states to the total C 1s spectrum (%) in transformation Blue CL- GQDs #Glycine structure on Ag electrodes under electrochemical reduction.

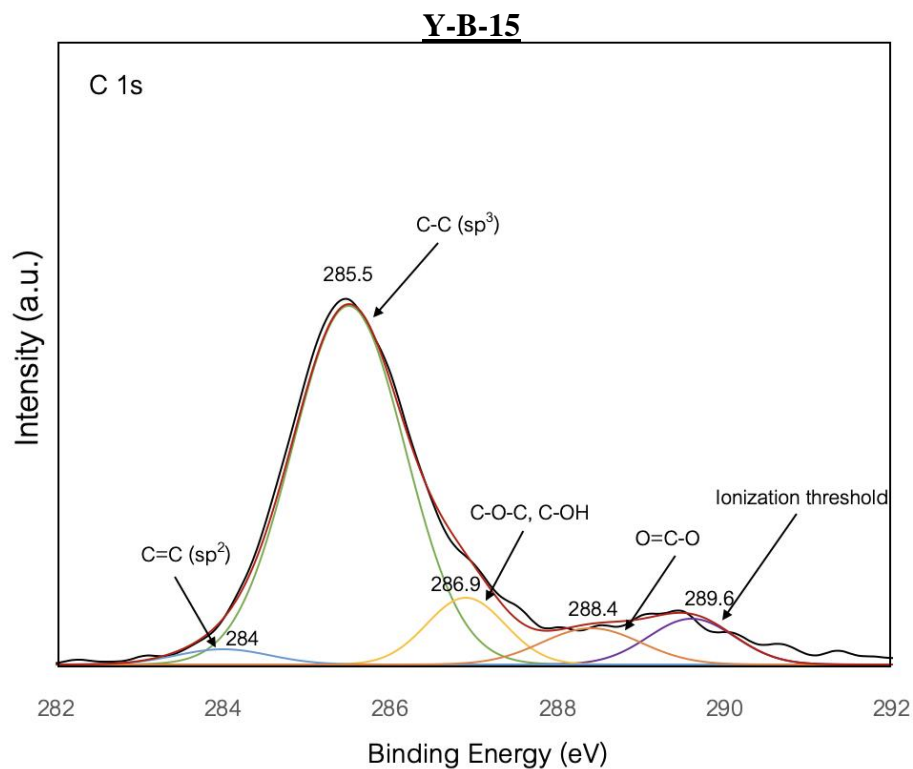
Sample	%sp²	%sp³	% Oxygenic functional group	sp³ to sp² ratio
B-G-15	3.67	72.95	14.87	19.90
B-G-30	3.50	80.73	8.27	23.09
B-G-45	4.11	77.35	14.70	18.81
B-G-60	3.32	78.90	9.55	23.75

After undergoing an additional 15-minute process, observations still revealed the presence of C=C, C-C, O=C-O, and Ionization threshold species detected at 284.4, 285.8, 287.9, and 289.8 eV, as shown in Figure 13 (b). There was an emergence of sp³, signifying an increase, and a decrease in the percentage of Oxygenic functional groups, as depicted in Table 8. Furthermore, an additional reduction in the percentage of carbon species bonded to oxygen atoms from 14.87 to 8.27% was observed, coupled with an increase in the sp³ to sp² ratio from 19.90 to 23.09, nearly 1.4 times higher. These findings suggest that the formation of supra carbon dots is facilitated by Ag NPs (nanoparticles) electrocatalysts, which deoxygenate the oxygenic functional groups, thereby forming sp³ C-C bonds.

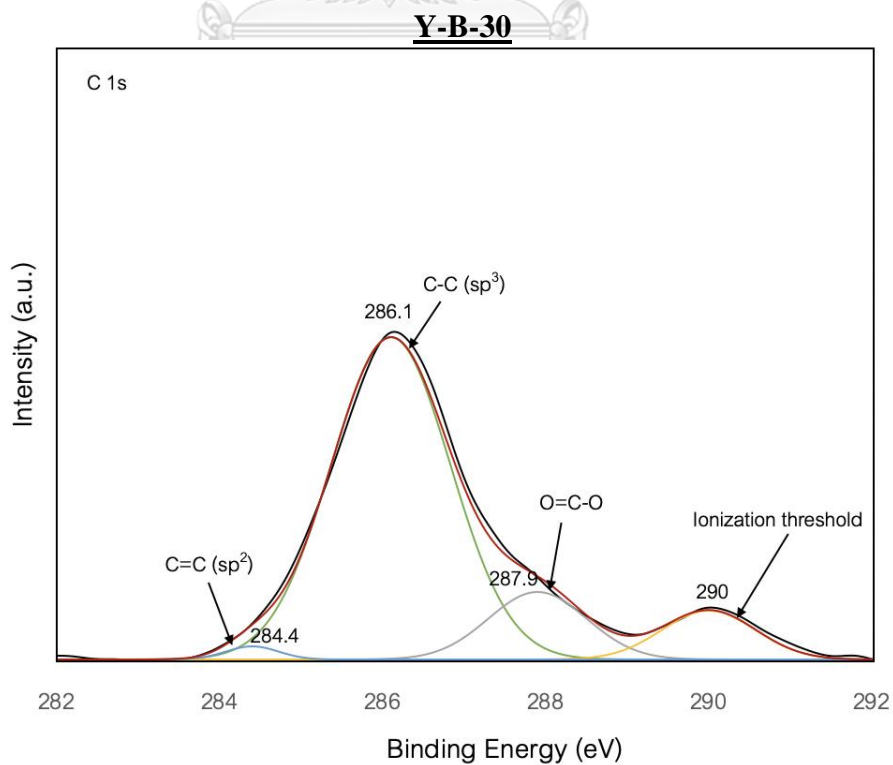
In the case of sample B-G-45, with an increased reaction time of 45 minutes, the carbon species observed in the XPS spectra are C=C, C-C, O=C-O, and Ionization threshold species detected at 284.6, 285.6, 287.9, and 289.9 eV, as shown in Figure 13 (c). There was an increase in the percentage of carbon species bonded to oxygen atoms from 8.27 to 14.70%, similar to that observed in B-G-15 at 15 minutes. However, this increase led to a decrease in the transformation of GQDs into supra carbon dots. Consequently, no transformation was observed on the outermost layer, but rather agglomeration of GQDs on that layer. This resulted in an increase in %sp² and an 18% decrease in the sp³ to sp² ratio from 23.09 to 18.81.

After undergoing an additional 15-minute process, observations still revealed the presence of C=C, C-C, O=C-O, and Ionization threshold species detected at 284.5, 286.1, 288.1, and 289.9 eV, as shown in Figure 13 (d). An emergence of sp³ was observed, signifying an increase, suggesting additional deoxygenation and transformation processes with an increased reaction time. This led to a decrease in the percentage of Oxygenic functional groups, as depicted in Table 8. Furthermore, there was an additional reduction in the percentage of carbon species bonded to oxygen atoms from 14.70 to 9.55%, coupled with an increase in the sp³ to sp² ratio from 18.81 to 23.75, almost 1.3 times higher.

4.2.3 X-ray Photoelectron Spectroscopy of Yellow CL- GQDs #Bicarbonate different times (5, 30, 45 and 60 min.)



(a)



(b)

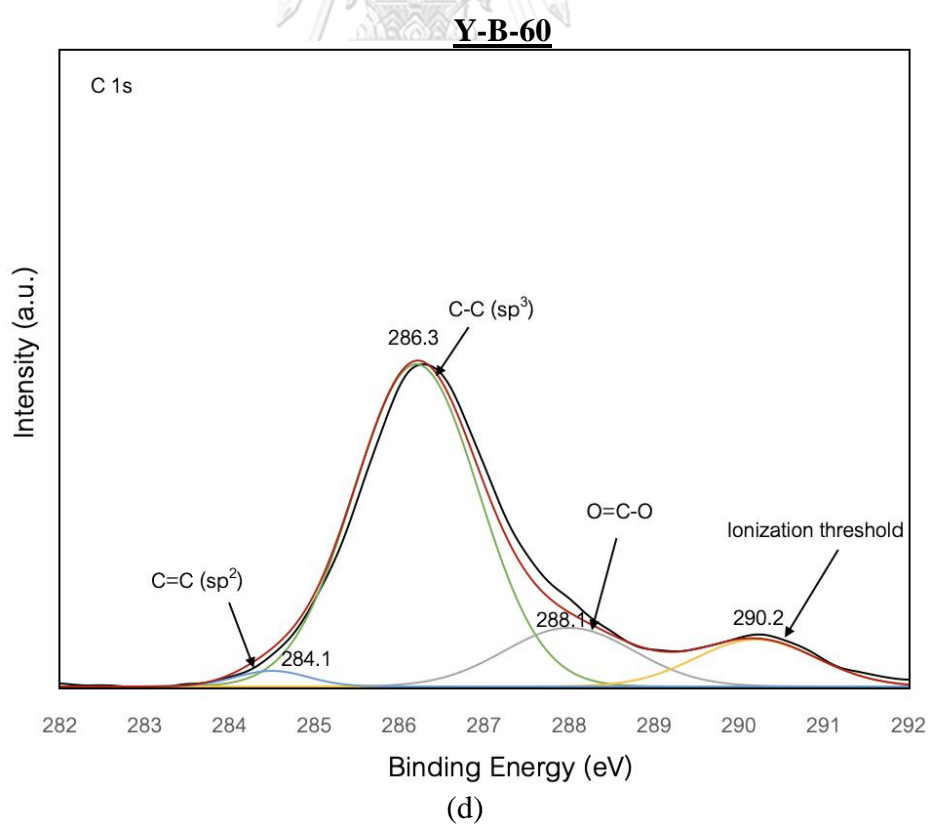
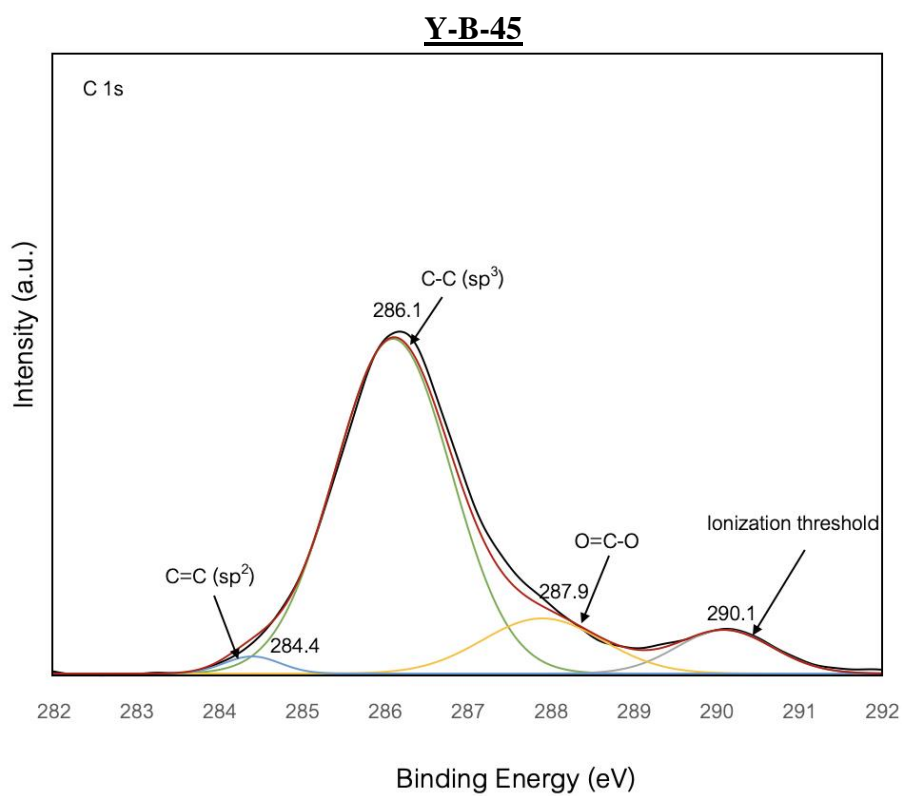


Figure 14 XPS image of Yellow CL- GQDs #Bicarbonate different times: (a) 15 minutes (b) 30 minutes (c) 45 minutes (d) 60 minutes

Table 9 Contribution of carbon states to the total C 1s spectrum (%) in transformation Yellow CL- GQDs #Bicarbonate structure on Ag electrodes under electrochemical reduction.

Sample	%sp²	%sp³	% Oxygenic functional group	Sp³ to sp² ratio
Y-B-15	2.72	73.62	16.44	27.05
Y-B-30	1.43	76.08	13.29	53.10
Y-B-45	1.94	76.82	13.06	39.51
Y-B-60	2.12	73.63	13.78	34.73

At Y-B-15 the reaction time of 15 min, From Figure 14 (a). XPS spectra demonstrates C=C, C-C, C-O-C or C-OH, O=C-O and Ionization threshold species detected at 284, 285.5, 286.9, 288.4 and 289.9 eV, respectively. The sp³ to sp² ratio and the percentage of carbon species bonded to oxygen atoms in supra carbon dots upon running the reaction for 15 min was calculated to be 27.05 and 16.44%. at table 9.

Having been further proceeded for another 15 min, there were still observation of C=C, C-C, O=C-O and Ionization threshold species detected at 284.4, 286.1, 287.9 and 290 eV, with the disappear of the peak at 286.9 eV show at the figure 14 (b), resulting in almost two times increase in the sp³ to sp² ratio from 27.05 to 53.10, the significant drop of the percentage of carbon species bonded to oxygen atoms from 16.44 to 13.29% suggests that the formation of supra carbon dots are proceeded by Ag NPs (nano particle) electrocatalyst deoxygenating the oxygenic functional groups.

For the sample Y-B-45 By increasing the reaction time to 45 min, the carbon species observed in XPS spectra are C=C, C-C, O=C-O and Ionization threshold species detected at 284.4, 286.1, 287.9 and 290.1 eV, show at the figure 14 (c). Additional reduction of the percentage of carbon species bonded to oxygen atoms from 13.29 to 13.06% with the It hasn't changed much from the Y-B-30. The decrease 25% in sp³ to sp² ratio from 53.10 to 39.51, Due to the significant amount of supra carbon dots on the cathode preventing the contact between upcoming GQDs and Ag NP electrocatalyst, the transformation of GQDs into supra carbon dots is decrease, resulting in no transformation step on the outmost layer, but rather GQDs agglomeration on the layer resulting in %sp² increase and decrease in sp³ to sp² ratio.

For the sample Y-B-60 By increasing the reaction time to 60 min, the carbon species observed in XPS spectra are the same as in case of Y-B-45 at 45 min with a slight shift in location. C=C, C-C, O=C-O and Ionization threshold species detected at 284.1, 286.3, 288.1 and 290.2 eV, show at the figure 9 (d).The resulted are the same as in case of Y-B-45 with %sp² increase and decrease in sp³ to sp² ratio. The decrease 12% in sp³ to sp² ratio from 39.51 to 34.73.

4.3 Characterization of the sample by Raman spectroscopy

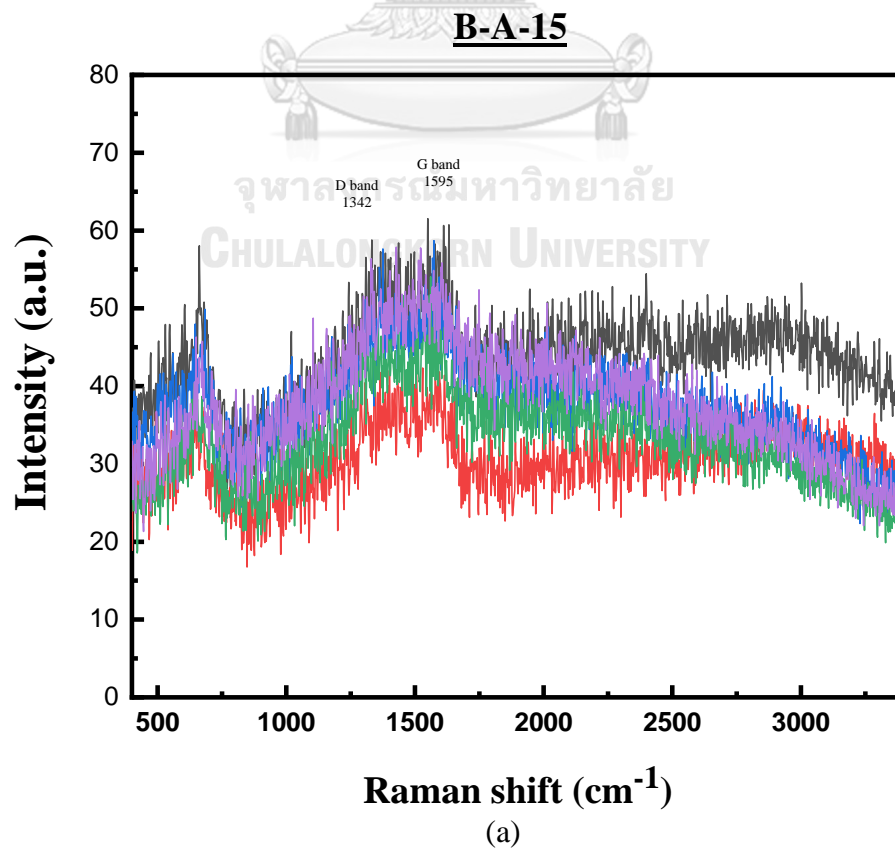
4.3.1 Raman spectroscopy of Blue CL- GQDs #Acetic different times (5, 30, 45 and 60 min.)

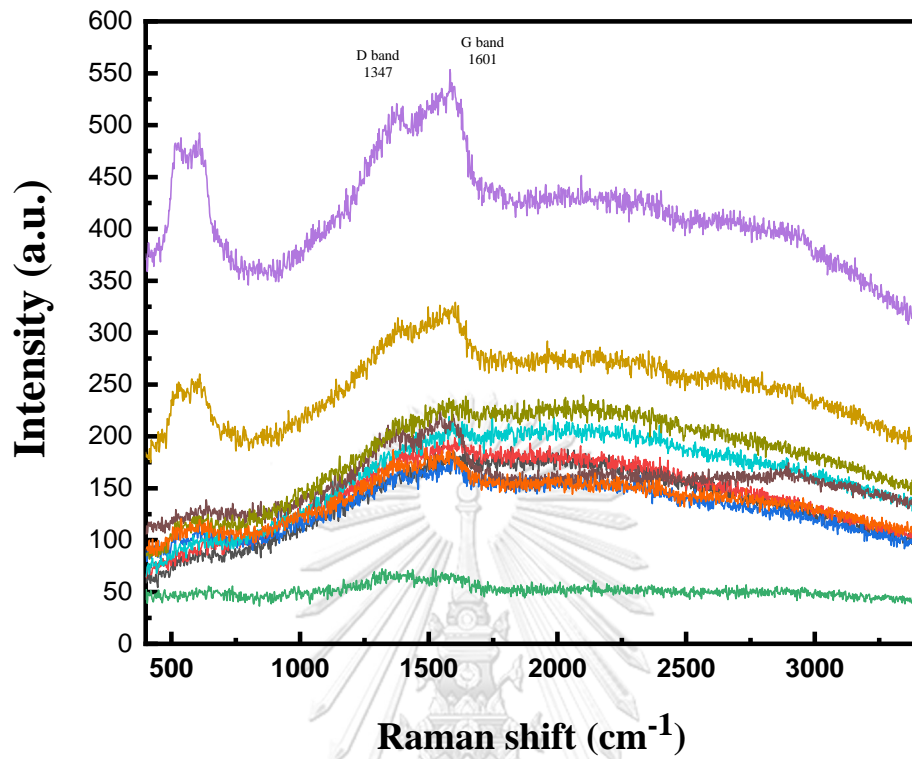
According to Raman spectroscopy the peaks while the broadening in D band 1330 cm^{-1} and intensity is 56.4 a.u., the G band 1520 cm^{-1} and intensity is 57.8 a.u. Will have a IG/ID ratio equal to 1.024 show in Figure 15 (a).

According to Raman spectroscopy the peaks while the broadening in D band 1380 cm^{-1} and intensity is 510 a.u., the G band 1601 cm^{-1} and intensity is 536 a.u. Will have a IG/ID ratio equal to 1.050 show in Figure 15 (b).

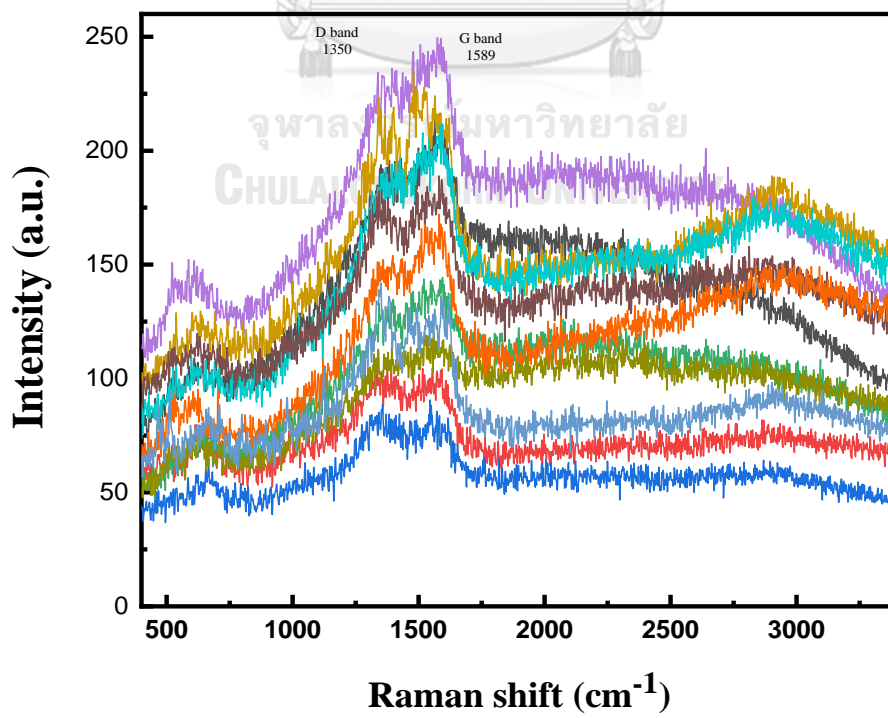
According to Raman spectroscopy the peaks while the broadening in D band 1350 cm^{-1} and intensity is 232 a.u., the G band 1590 cm^{-1} and intensity is 249 a.u. Will have a IG/ID ratio equal to 1.073 show in Figure 15 (C).

According to Raman spectroscopy the peaks while the broadening in D band 1380 cm^{-1} and intensity is 840 a.u., the G band 1590 cm^{-1} and intensity is 922 a.u. Will have a IG/ID ratio equal to 1.097 show in Figure 15 (d).



B-A-30

(b)

B-A-45

(c)

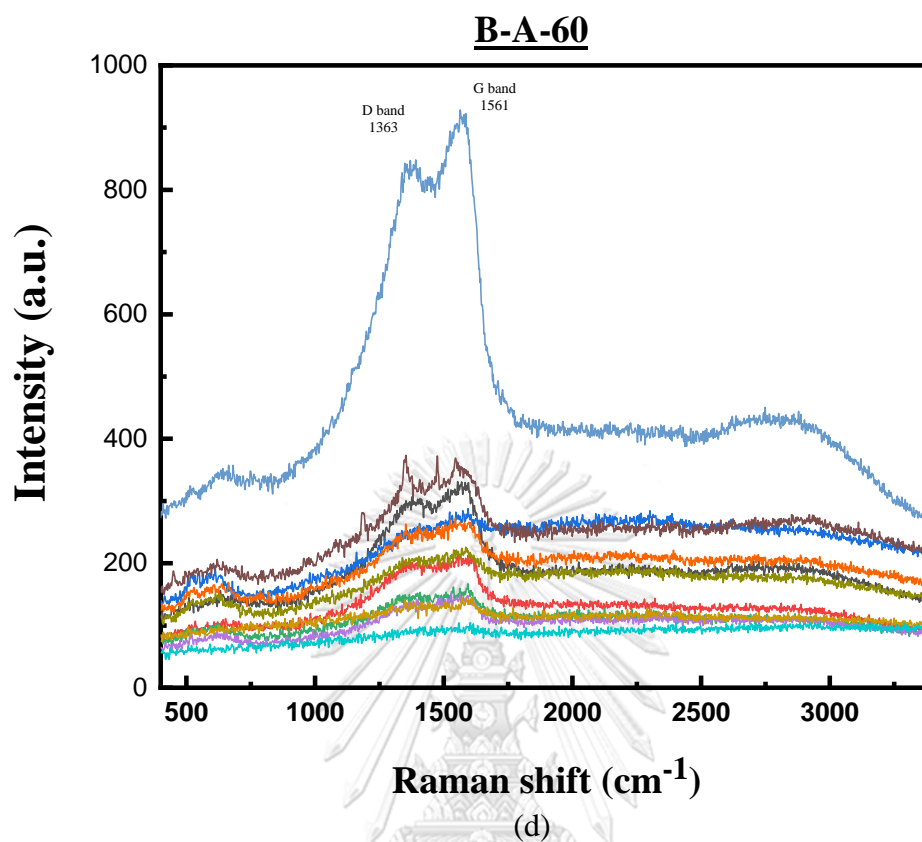


Figure 15 Raman spectroscopy image of Blue CL- GQDs #Acetic different times:
 (a) 15 minutes (b) 30 minutes (c) 45 minutes (d) 60 minutes

Table 10 IG/ID ratio of Blue CL- GQDs #Acetic

Sample	D band	G band	ID	IG	IG/ID ratio
B-A-15	1330	1520	56.4	57.8	1.024
B-A-30	1380	1601	510	536	1.050
B-A-45	1350	1590	232	249	1.073
B-A-60	1380	1590	840	922	1.097

The D band is indicative of defects or edges in the sample. The ratio of the intensity of the D band, ($\sim 1350 \text{ cm}^{-1}$) to that of the G band ($\sim 1590 \text{ cm}^{-1}$) band indicates the structure, size, and defects of the carbon material. ID/IG ratio was measured as

shown in Table 10. B-A-30 would show a higher ID/IG ratio followed by B-A-45, B-A-60, and B-A-15 respectively.

The intensity ratio of G band to D band (IG / ID ratio) is used as an indicator of the amount of defects. If the IG / ID ratio is large, it can be judged that the carbon material have few defects, and if the IG / ID ratio is small, they are carbon material having many defects. This suggests that B-A-30 have few defects. followed by B-A-45, B-A-60, and B-A-15 respectively.

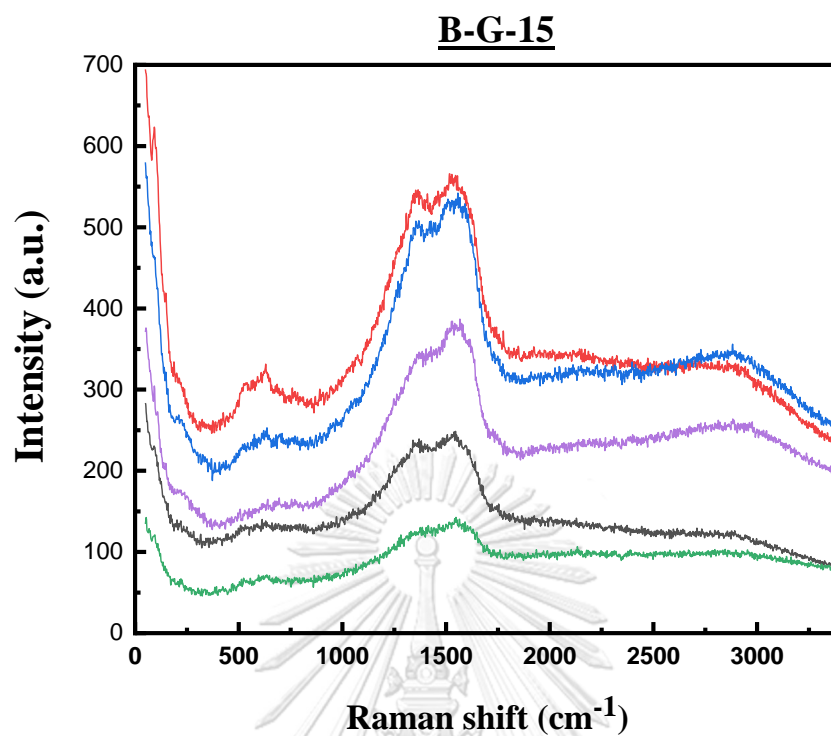
4.3.2 Raman spectroscopy of Blue CL- GQDs #Glycine different times (5, 30, 45 and 60 min.)

According to Raman spectroscopy the peaks while the broadening in D band 1380 cm^{-1} and intensity is 501 a.u., the G band 1570 cm^{-1} and intensity is 537 a.u. Will have a IG/ID ratio equal to 1.072 show in Figure 16 (a).

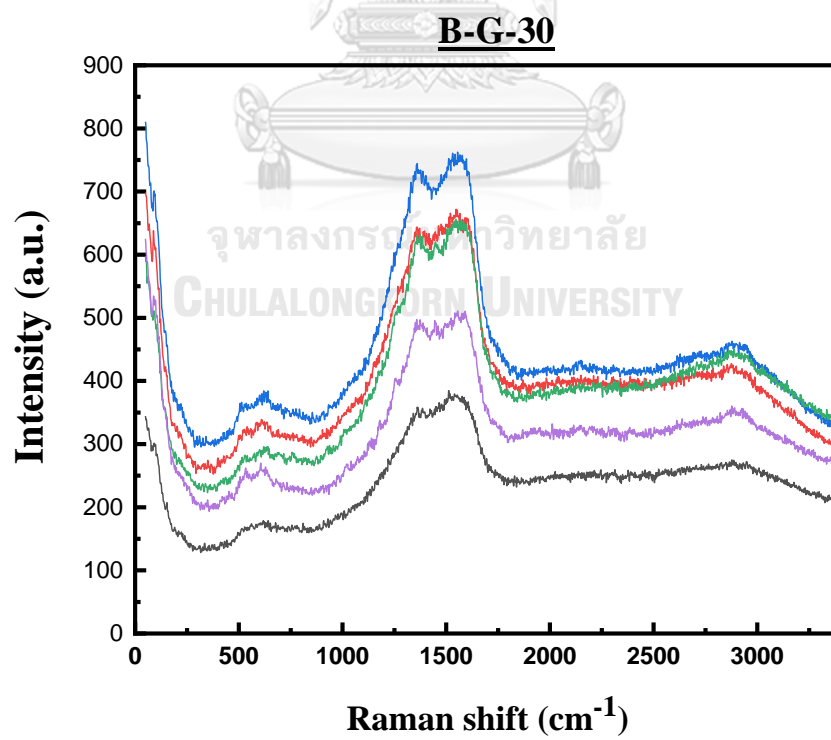
According to Raman spectroscopy the peaks while the broadening in D band 1380 cm^{-1} and intensity is 733 a.u., the G band 1580 cm^{-1} and intensity is 748 a.u. Will have a IG/ID ratio equal to 1.02 show in Figure 16 (b).

According to Raman spectroscopy the peaks while the broadening in D band 1390 cm^{-1} and intensity is 525 a.u., the G band 1580 cm^{-1} and intensity is 568 a.u. Will have a IG/ID ratio equal to 1.082 show in Figure 16 (c).

According to Raman spectroscopy the peaks while the broadening in D band 1390 cm^{-1} and intensity is 137 a.u., the G band 1580 cm^{-1} and intensity is 153 a.u. Will have a IG/ID ratio equal to 1.117 show in Figure 16 (d).



(a)



(b)

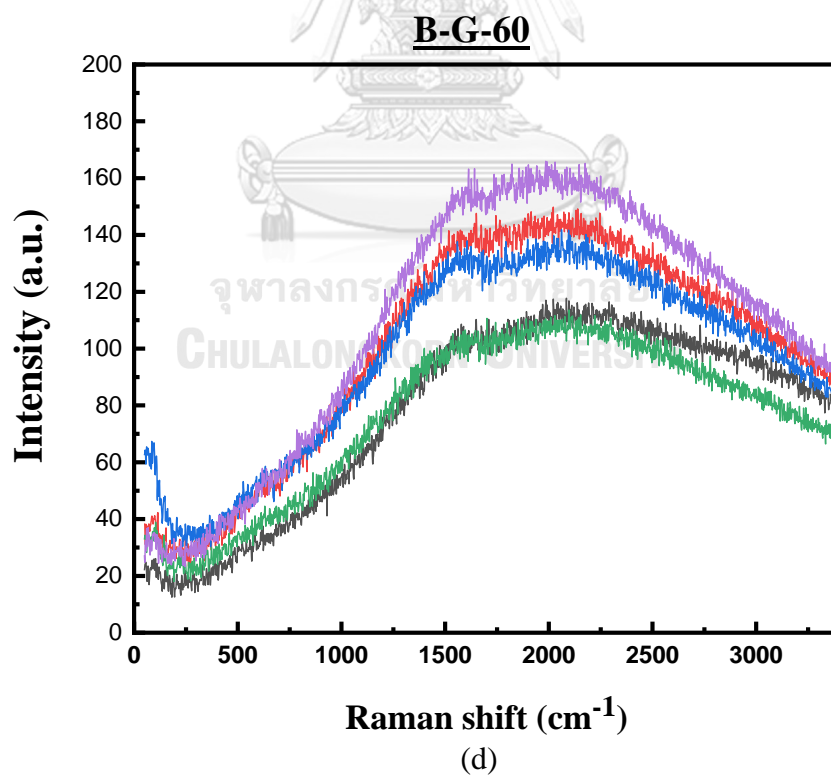
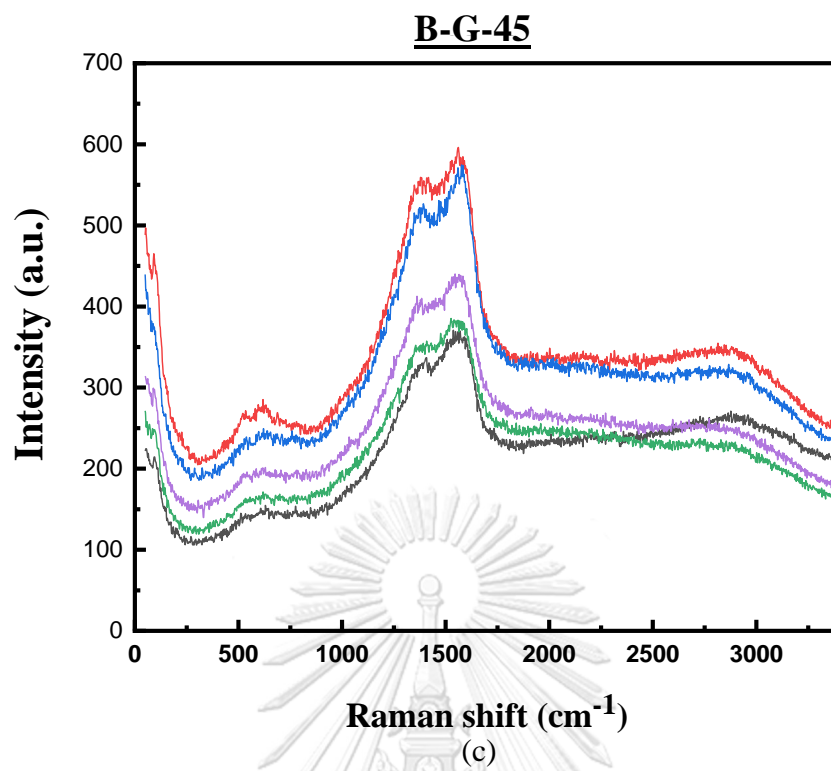


Figure 16 Raman spectroscopy image of Blue CL- GQDs #Glycine different times: (a) 15 minutes (b) 30 minutes (c) 45 minutes (d) 60 minutes.

Table 11 IG/ID ratio of Blue CL- GQDs # Glycine

Sample	D band	G band	ID	IG	IG/ID ratio
B-G-15	1380	1570	501	537	1.072
B-G-30	1380	1580	733	748	1.020
B-G-45	1390	1580	525	568	1.082
B-G-60	1390	1580	137	153	1.117

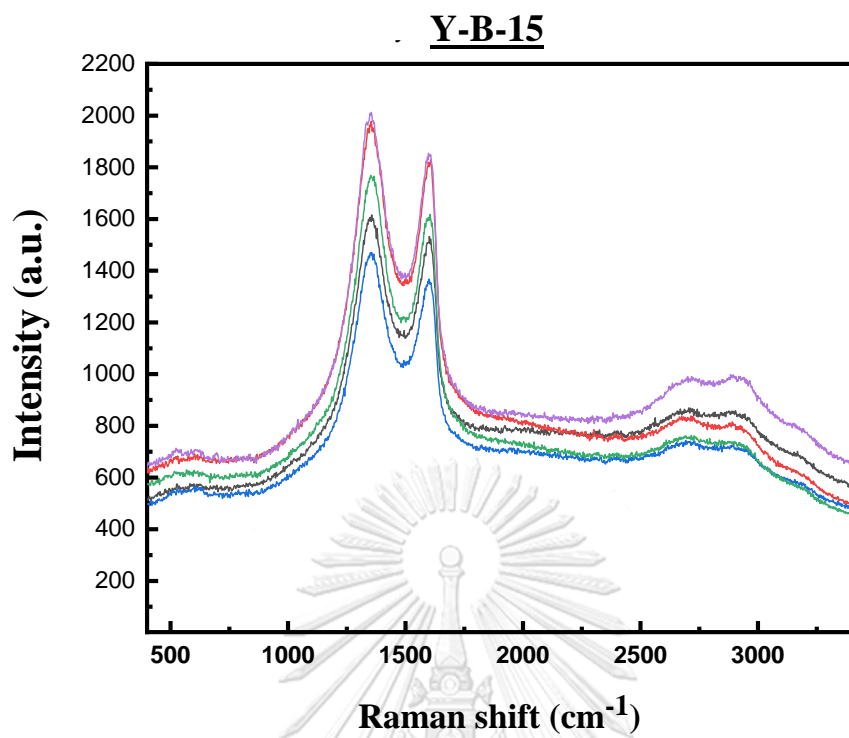
4.3.3 Raman spectroscopy of Yellow CL- GQDs #Bicarbonate different times (5, 30, 45 and 60 min.)

According to Raman spectroscopy the peaks while the broadening in D band 1360 cm^{-1} and intensity is 1,980 a.u., the G band 1610 cm^{-1} and intensity is 1,820 a.u. Will have a IG/ID ratio equal to 0.919 show in Figure 17 (a).

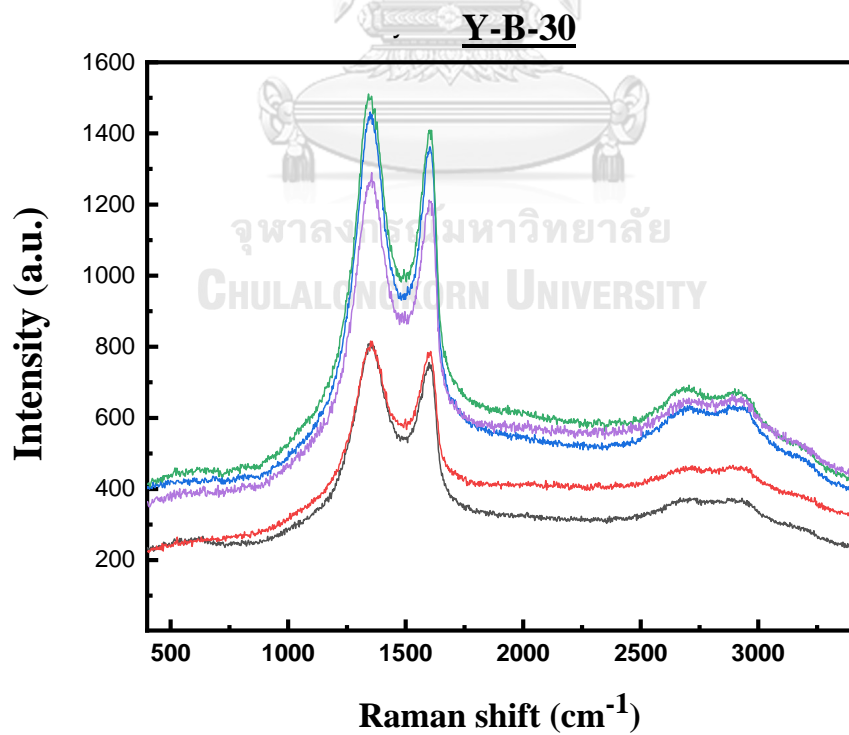
According to Raman spectroscopy the peaks while the broadening in D band 1370 cm^{-1} and intensity is 1,470 a.u., the G band 1610 cm^{-1} and intensity is 1,370 a.u. Will have a IG/ID ratio equal to 0.932 show in Figure 17 (b).

According to Raman spectroscopy the peaks while the broadening in D band 1370 cm^{-1} and intensity is 13,600 a.u., the G band 1580 cm^{-1} and intensity is 12,600 a.u. Will have a IG/ID ratio equal to 0.926 show in Figure 17 (c).

According to Raman spectroscopy the peaks while the broadening in D band 1370 cm^{-1} and intensity is 3,690 a.u., the G band 1610 cm^{-1} and intensity is 3,380 a.u. Will have a IG/ID ratio equal to 0.916 show in Figure 17 (d).



(a)



(b)

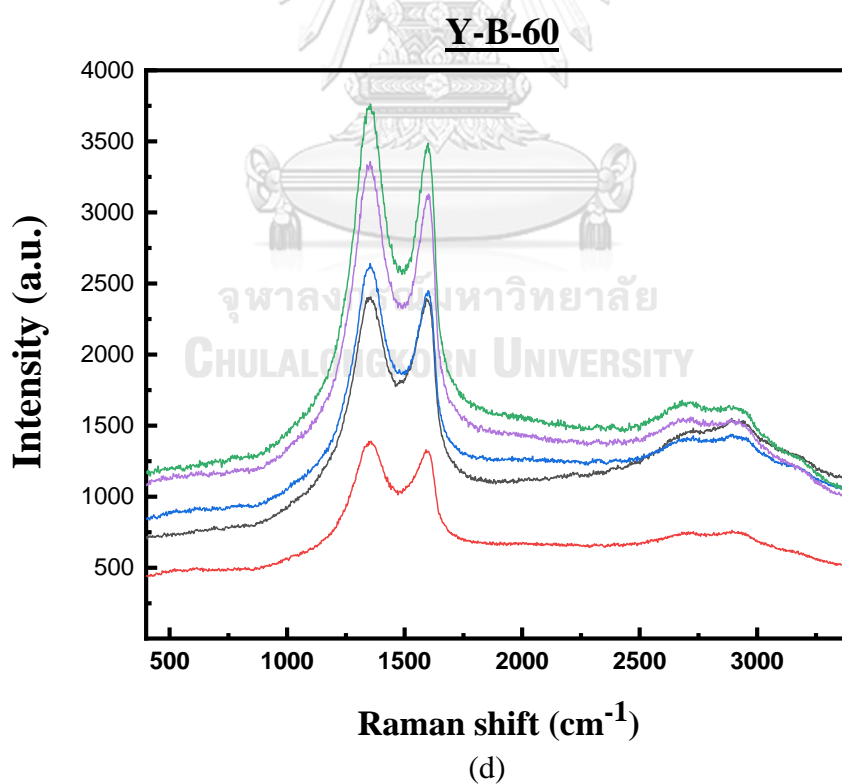
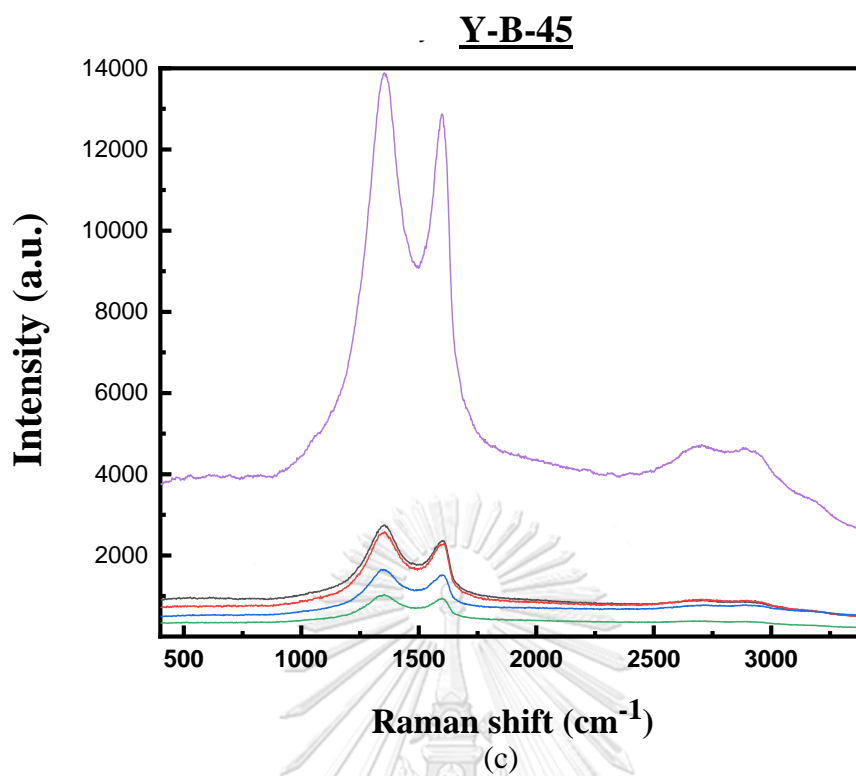


Figure 17 Raman spectroscopy image of Yellow CL- GQDs #Bicarbonate different times: (a) 15 minutes (b) 30 minutes (c) 45 minutes (d) 60 minute.

Table 12 IG/ID ratio of Blue CL- GQDs # Bicarbonate

Sample	D band	G band	ID	IG	IG/ID ratio
Y-B-15	1360	1610	1980	1820	0.919
Y-B-30	1370	1610	1470	1370	0.932
Y-B-45	1370	1610	13600	12600	0.926
Y-B-60	1370	1610	3690	3380	0.916



Part II. To investigate the effects of GQDs particle for applied in screen printed electrodes, by using the better condition from the first objective, on the characteristics Cyclic voltammetry.

4.4 Electrochemical characterization of GQDs

4.4.1 Application of Blue CL- GQDs #Acetic, Derived transforming graphene quantum dot structure on Ag electrodes under electrochemical reduction in Electrochemical Sensor.

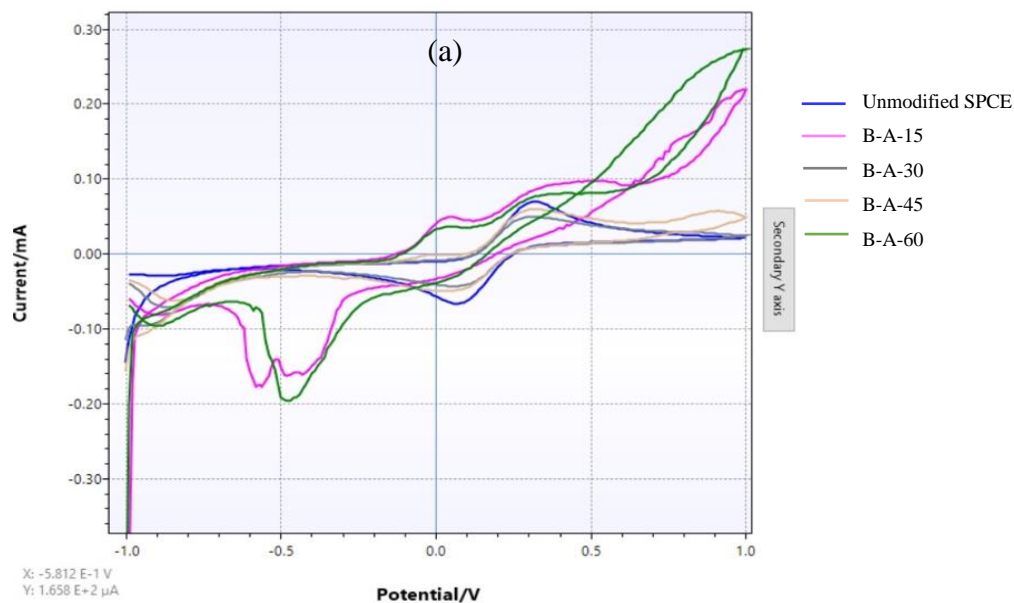


Figure 18 Illustration of Blue CL- GQDs #Acetic modified SPCE for electrochemical sensor application, Cyclic voltammograms of 5.0 mM $[Fe(CN)_6]^{3-/4-}$ in 0.1 M KCl measured on different electrodes at a scan rate of 100 mVs^{-1} , and the corresponding peak current extracted from the CVs ($n=3$).

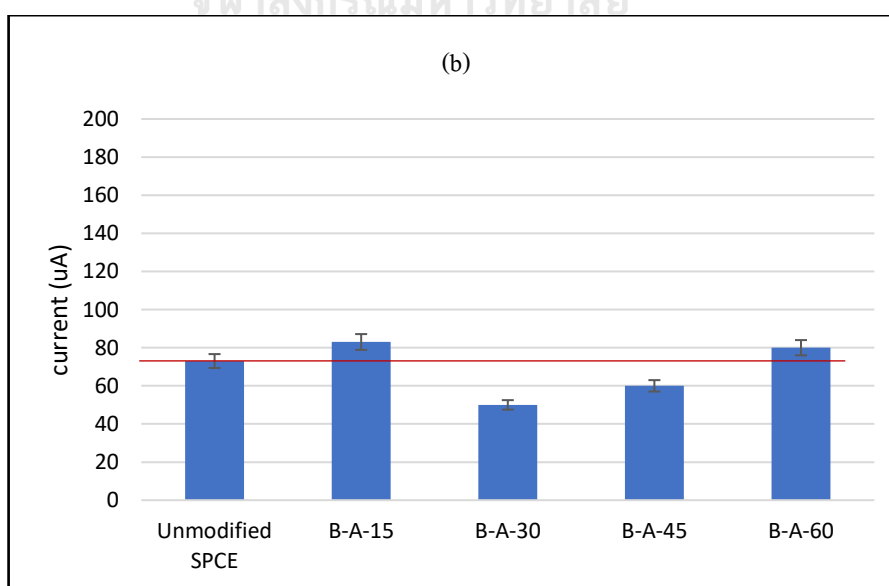


Figure 19 Illustration of Blue CL- GQDs #Acetic modified SPCE for electrochemical sensor application, show the current at potential 0.1 V

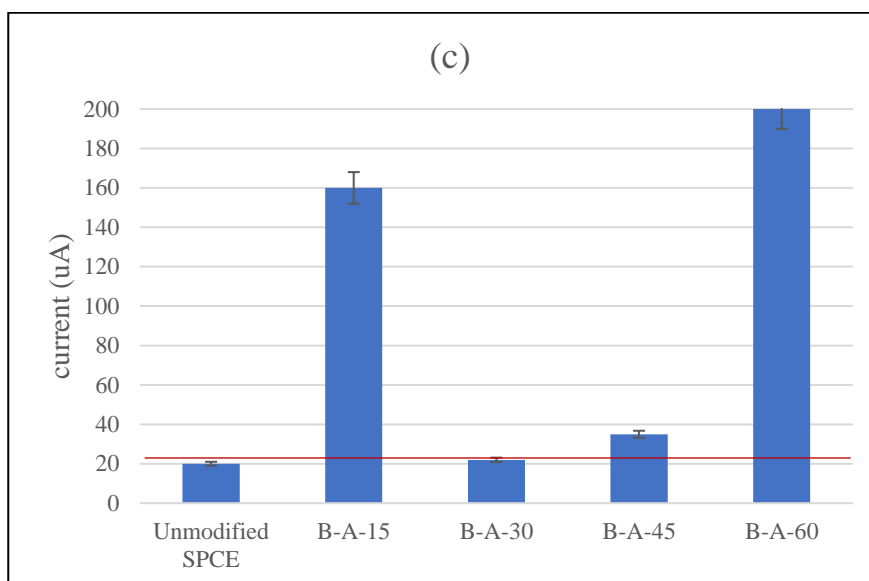


Figure 20 Illustration of Blue CL- GQDs #Acetic modified SPCE for electrochemical sensor application, show the current at potential -0.48 V

In the potential application of utilizing Graphene (Blue CL-GQDs #Acetic) and transforming the graphene quantum dot structure on Ag electrodes as an additive in electrochemical sensors, the sample was dispersed in N,N-dimethylformamide using an ultrasonicator for 2 hours. Subsequently, 3 μ L of the composite was directly applied to the working electrode area of a screen-printed carbon electrode (SPCE), depicted in Figure 18. Through cyclic voltammetry, the current response signal of a standard redox couple ferri/ferrocyanide ($[\text{Fe}(\text{CN})_6]^{3-/4-}$) was observed. Test results indicated that samples B-A-15 and B-A-60 produced similar curve peaks, while samples B-A-30 and B-A-45 exhibited analogous curve peaks, as illustrated in Fig. 18. However, at the potential 0.3 V, all of them displayed a smaller response compared to the unmodified polarity, as shown in Fig. 19. This outcome might be attributed to their low dispersibility in the solvent, resulting in larger particle sizes and agglomeration. Consequently, this agglomeration caused blockages at the electrodes, inhibiting effective electron conduction.

However, when observing at the potential -0.48 V, it was found that the samples B-A-15, B-A-60 response than B-A-30, B-A-45 and almost nine times current increase in unmodified SPCE as shown in Fig.20

4.4.2 Application of Blue CL- GQDs #Glycine, Derived transforming graphene quantum dot structure on Ag electrodes under electrochemical reduction in Electrochemical Sensor.

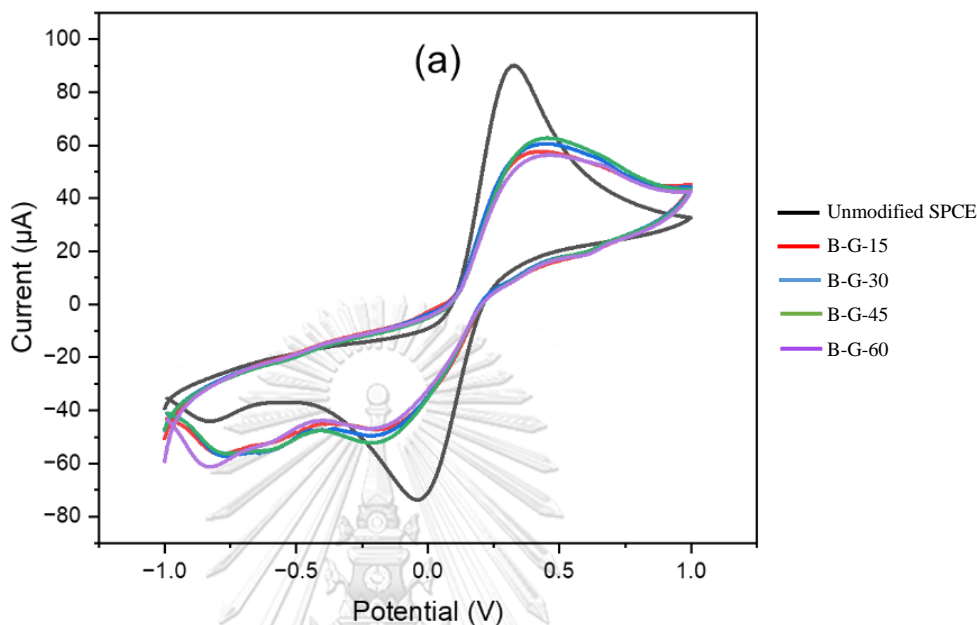


Figure 21 Illustration of Blue CL- GQDs #Glycine modified SPCE for electrochemical sensor application, Cyclic voltammograms of 5.0 mM $[Fe(CN)_6]^{3-/4-}$ in 0.1 M KCl measured on different electrodes at a scan rate of 100 mVs^{-1} , and the corresponding peak current extracted from the CVs ($n=3$).

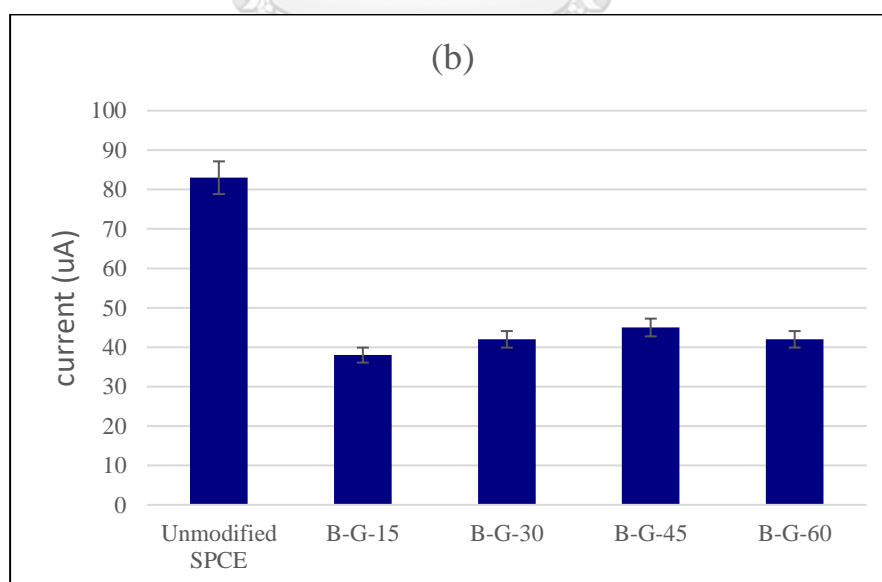


Figure 22 Illustration of Blue CL- GQDs #Glycine modified SPCE for electrochemical sensor application, show the current at potential 0.3 V

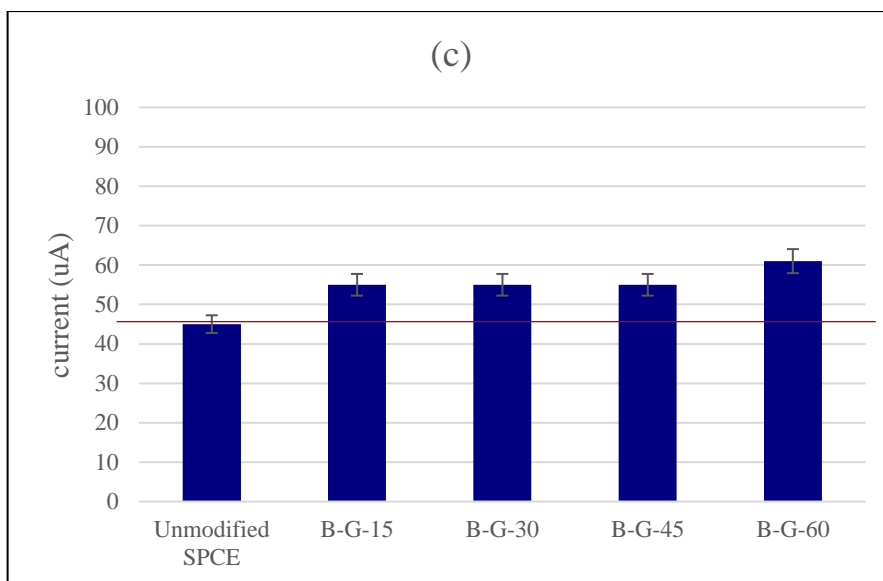


Figure 23 Illustration of Blue CL- GQDs #Glycine modified SPCE for electrochemical sensor application, show the current at potential -0.8 V

In the potential application of utilizing Graphene (Blue CL-GQDs #Glycine) and transforming the graphene quantum dot structure on Ag electrodes as an additive in electrochemical sensors, the sample was dispersed in N,N-dimethylformamide using an ultrasonicator for 2 hours. Subsequently, 3 μL of the composite was directly applied to the working electrode area of a screen-printed carbon electrode (SPCE), depicted in Figure 21. Through cyclic voltammetry, the current response signal of a standard redox couple ferri/ferrocyanide ($[\text{Fe}(\text{CN})_6]^{3-/4-}$) was observed. Test results indicated that samples B-A-15, B-A-30, B-A-45, and B-A-60 produced similar curve peaks, as shown in Fig. 21. However, at the potential 0.3 V, all of them exhibited a smaller response compared to the unmodified polarity, as shown in Fig. 22. This outcome might be due to their low dispersibility in the solvent, leading to easy precipitation and larger particle sizes, resulting in agglomeration. This agglomeration caused blockages at the electrodes, hindering effective electron conduction. Notably, B-G-15 exhibited the best dispersion among different times.

However, upon observing at the potential of -0.8 V, it was observed that samples B-A-15, B-A-30, B-A-45, and B-A-60 all exhibited a smaller response compared to the unmodified SPCE, approximately 20%, as shown in Fig. 23.

4.4.3 Application of Yellow CL- GQDs #Bicarbonate, Derived transforming graphene quantum dot structure on Ag electrodes under electrochemical reduction in Electrochemical Sensor.

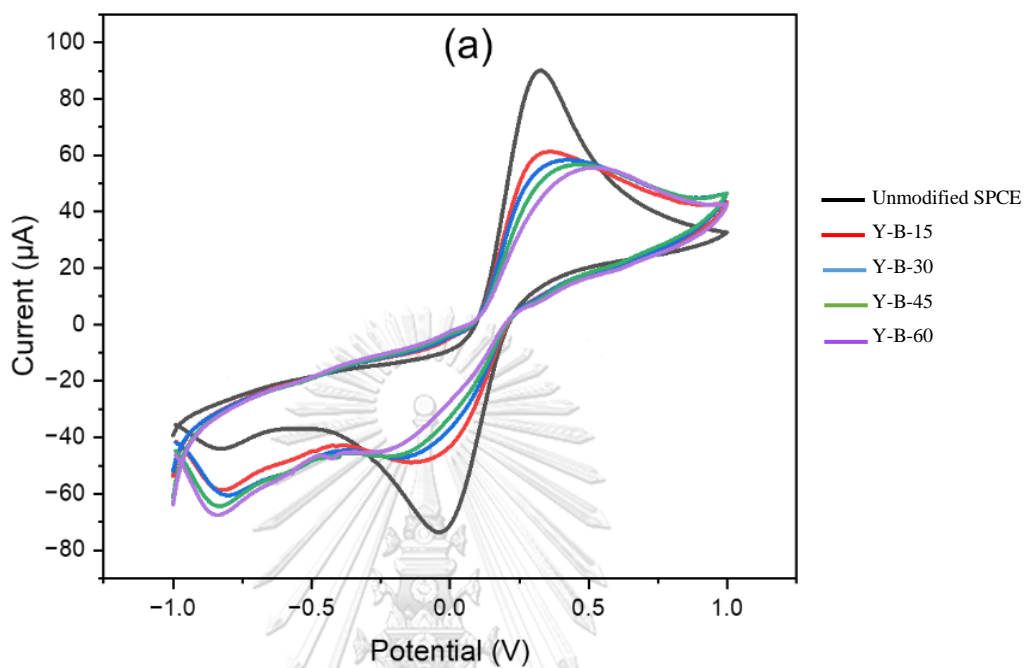


Figure 24 Illustration of Yellow CL- GQDs #Bicarbonate modified SPCE for electrochemical sensor application, Cyclic voltammograms of 5.0 mM $[Fe(CN)_6]^{3-/4-}$ in 0.1 M KCl measured on different electrodes at a scan rate of 100 mVs^{-1} , and the corresponding peak current extracted from the CVs ($n=3$).

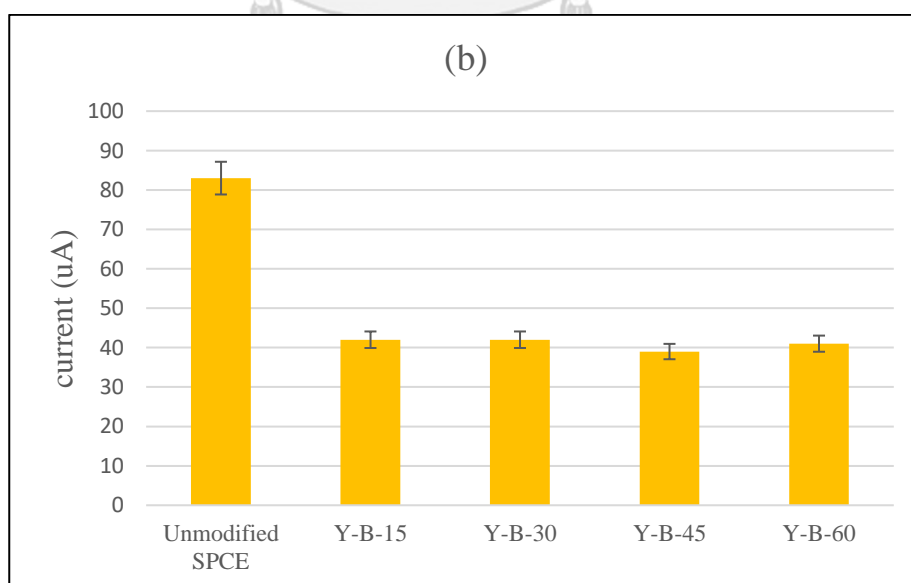


Figure 25 Illustration of Yellow CL- GQDs #Bicarbonate modified SPCE for electrochemical sensor application, , show the current at potential 0.3 V

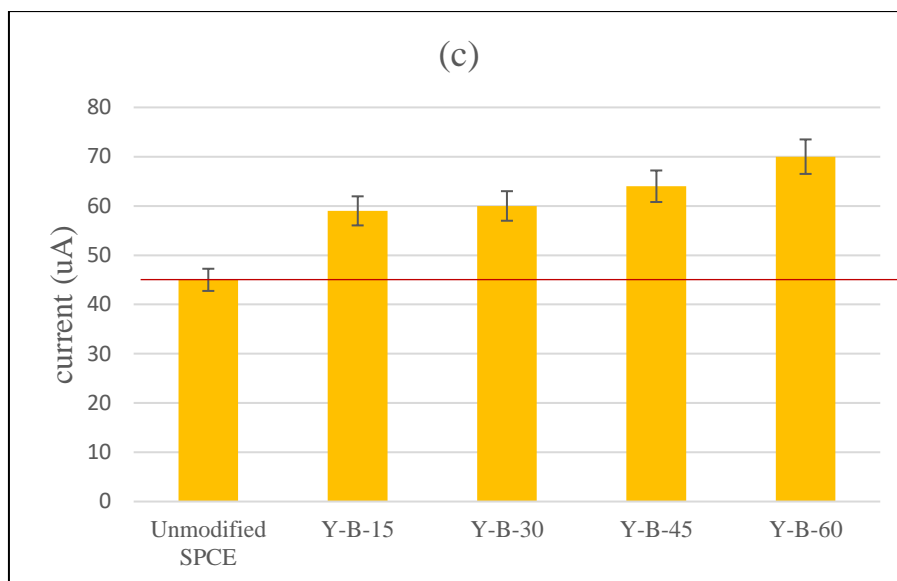


Figure 26 Illustration of Yellow CL- GQDs #Bicarbonate modified SPCE for electrochemical sensor application, show the current at potential -0.8 V

In the potential application of utilizing Graphene (Yellow CL-GQDs #Bicarbonate) and transforming the graphene quantum dot structure on Ag electrodes as an additive in electrochemical sensors, the sample was dispersed in N,N-dimethylformamide using an ultrasonicator for 2 hours. Subsequently, $3\ \mu\text{L}$ of the composite was directly applied to the working electrode area of a screen-printed carbon electrode (SPCE), as depicted in Figure 24. Cyclic voltammetry was employed to observe the current response signal of a standard redox couple ferri/ferrocyanide ($[\text{Fe}(\text{CN})_6]^{3-/4-}$). According to the test results, samples B-A-15, B-A-30, B-A-45, and B-A-60 produced similar curve peaks, as shown in Fig. 24. However, at the potential of 0.3 V , all of them exhibited a smaller response compared to the unmodified polarity, as illustrated in Fig. 25. This outcome might be attributed to their low dispersibility in the solvent, easy precipitation, large particle size, and agglomeration. Consequently, this agglomeration caused blockages at the electrodes, impeding effective electron conduction.

However, upon observation at the potential of -0.8 V , it was found that samples B-A-15, B-A-30, B-A-45, and B-A-60 all exhibited a smaller response, about 32% lower than the unmodified SPCE. Notably, B-A-60 showed the best response, as illustrated in Fig. 26.

CHAPTER V

CONCLUSIONS

5.1 Conclusions

The results of the Electrochemical characterization of Blue CL-GQDs #Acetic by cyclic voltammetry indicated that both the B-A-15 sample at 15 minutes and the B-A-60 sample at 60 minutes exhibited the highest current. This suggests their potential suitability for assessing the quality of the screen-printed electrode. SEM-EDX images showed that both B-A-15 and B-A-60 had a smooth thin film morphology, contributing to their higher current in cyclic voltammetry. However, samples B-A-30 and B-A-45 displayed lower currents. This can be attributed to their SEM-EDX-observed 3D structure, leading to larger particles that easily settle and poorly disperse, thereby reducing the current.

Furthermore, XPS results from samples B-A-15 and B-A-60 indicated a higher percentage of sp² compared to B-A-30 and B-A-45. This higher sp² structure in graphene quantum dots, characterized by double bonds between atoms, enhances electron mobility. In contrast, the sp³ structure found in B-A-30 and B-A-45, characterized by single bonds, results in lower electron mobility. The increased electron mobility in the sp² structure allows for better electrical conductivity as electrons can move more freely through the structure.

The Electrochemical characterization results from cyclic voltammetry for the Blue CL-GQDs #Glycine sample indicated similar currents across all samples, showing no significant differences. This similarity in current can be attributed to the SEM-EDX images, which displayed a uniform smooth thin film morphology across all samples. Additionally, the XPS analysis revealed a relatively low percentage of sp², which leads to poor electron mobility. Consequently, all Blue CL-GQDs #Glycine samples exhibited lower currents compared to the unmodified sample.

Finally, the Yellow CL-GQDs #Bicarbonate sample, upon Electrochemical characterization via cyclic voltammetry, exhibited similar results to those of the Blue CL-GQDs #Glycine sample. All conditions showed similar current responses. SEM-EDX analysis indicated a consistent 3D structure across these samples with large particles that were challenging to disperse. XPS results also showed uniformly low percentages of sp², resulting in poor current performance in cyclic voltammetry when compared to the unmodified sample.

However, when applying a potential of -0.8 V, samples B-G-15, B-G-30, B-G-45, B-G-60, Y-B-15, Y-B-30, Y-B-45, Y-B-60, all exhibited a higher current response compared to the unmodified sample. This suggests the potential for their application in other future applications.

The results indicate that the electrochemical reduction time has varying effects on the characteristics of GQDs prepared through electrochemical reduction on Ag electrodes. The samples from Blue CL-GQDs #Acetic at 15 minutes and 60 minutes exhibited the highest current, surpassing those from Blue CL-GQDs #Glycine, Yellow CL-GQDs #Bicarbonate, and the unmodified sample. This suggests their suitability for application in screen-printed electrodes [11-18]

5.2 Recommendations

1. It might be advisable to utilize other GQDs, such as green, orange, or red fluorescent ones, to compare their performance for potential application in screen-printed electrodes.
2. Considering the high current observed in the results from Blue CL-GQDs #Glycine and Yellow CL-GQDs #Bicarbonate at -0.8V, further studies should be conducted to explore their suitability for alternative applications.

REFERENCES

1. Geim, A.K., *Graphene: status and prospects*. Science 324(5934), 2009: p. 1530-1534.
2. Zheng, X.T., *Glowing graphene quantum dots and carbon dots : properties, syntheses, and biological applications*. . Small 11(14), 1620–1636., 2015.
3. Li, Q.Z., *Nitrogen-doped colloidal graphene quantum dots and their size-dependent electrocatalytic activity for the oxygen reduction reaction*. . Journal of the American Chemical Society 134(46), 2012: p. 18932–18935.
4. Pan, D.Z., *Hydrothermal route for cutting graphene sheets into blue-luminescent graphene quantum dots*. Advanced Materials 22(6), 2010: p. 734–738.
5. Lerato L. Mokoloko, R.P., *The Transformation of 0-D Carbon Dots into 1-, 2- and 3-D Carbon Allotropes*. A Minireview. Nanomaterials 2515.
6. Liu, R.W., *Bottom-up fabrication of photoluminescent graphene quantum dots with uniform morphology*. . Journal of the American Chemical Society 133(39), 2011: p. 15221–15223.
7. Shinde, D.B., *Electrochemical resolution of multiple redox events for graphene quantum Dots*. . Angewandte Chemie - International Edition 52(9), 2482–2485., 2013.
8. Rungkiat Nganglumpoon, e.a., *Growing 3D-nanostructured carbon allotropes from CO₂ at room temperature under the dynamic CO₂ electrochemical reduction environment*. www.elsevier.com/locate/carbon, 241-255., 2022.
9. ชานินทร์ แดงวารัมย์, ม.ถ., การพัฒนาเคมีคอลเซนเซอร์สำหรับวัดตะกั่วในน้ำดื่ม ด้วยขั้วไฟฟ้าบีสมัทอะมัลกัม-ทองคำบอานาโนปรับแต่งด้วยโคโคซานแบบเชื่อมไขว้. มหาวิทยาลัยแม่โจ้, 2013: p. 1-133.
10. Piriya Pinthong, e.a., *Room Temperature Nanographene Production via CO₂ Electrochemical Reduction on the Electrodeposited Bi on Sn Substrate*. . Nanomaterials, 3389., 2022.
11. Fanjul-Bolado, P., et al., *Electrochemical characterization of screen-printed and conventional carbon paste electrodes*. Electrochimica Acta, 2008. **53**(10): p. 3635-3642.
12. Cheng, H., et al., *Graphene-Quantum-Dot Assembled Nanotubes: A New Platform for Efficient Raman Enhancement*. ACS nano, 2012. **6**: p. 2237-44.
13. García-Miranda Ferrari, A., S.J. Rowley-Neale, and C.E. Banks, *Screen-printed electrodes: Transitioning the laboratory in-to-the field*. Talanta Open, 2021. **3**: p. 100032.
14. Medeiros, G.A., C.V. da Silva Rodrigues, J. Spencer, and B.A.D. Neto, *7 - Carbon dots (C-dots): fluorescence processes and bioimaging*, in *Quantum Materials, Devices, and Applications*, M. Henini and M.O. Rodrigues, Editors. 2023, Elsevier. p. 201-213.
15. Shutthanandan, V., et al., *Applications of XPS in the characterization of Battery materials*. Journal of Electron Spectroscopy and Related Phenomena, 2019. **231**: p. 2-10.
16. Lomon, J., et al., *XPS and XAS preliminary studies of diamond-like carbon films prepared by HiPIMS technique*. Journal of Physics: Conference Series, 2018. **1144**: p. 012048.

17. Bharathi, G., et al., *Graphene Quantum Dot Solid Sheets: Strong blue-light-emitting & photocurrent-producing band-gap-opened nanostructures*. Scientific Reports, 2017. **7**.
18. Zhang, S., et al., *Construction of hierarchical porous carbon nanosheets from template-assisted assembly of coal-based graphene quantum dots for high performance supercapacitor electrodes*. Materials Today Energy, 2017. **6**: p. 36-45.



VITA

NAME Sivakorn Bovornsintuchon

DATE OF BIRTH 30 May 1996

PLACE OF BIRTH Chon buri, Thailand

**INSTITUTIONS
ATTENDED** B.Eng Chemical Engineering Faculty of Engineering,
King Mongkut's University of Technology North Bangkok.

HOME ADDRESS 109/30 Ban Bueng, Witoon Damri Road, Ban Bueng
District, Chonburi Province 20170



จุฬาลงกรณ์มหาวิทยาลัย
CHULALONGKORN UNIVERSITY